AN ELECTRICAL AND STATISTICAL STUDY OF BURST NOISE

Thesis by

Jason Niles Puckett, Jr.

In Partial Fulfillment of the Requirements

For the Degree of

Doctor of Philosophy

California Institute of Technology

Pasadena, California

1971

(Submitted October 27, 1970)

an die Anni

ACKNOWLEDGEMENTS

I should like to express my indebtedness to Dr. H. C. Martel for his guidance, perspicacious criticisms and suggestions. His moral support, moreover, was of great value throughout the period of this research. Dr. C. A. Mead merits thanks for numerous useful discussions and for recommendations regarding the initiation of the work. I am obligated to Dr. R. J. Whittier and Dr. S. T. Hsu of the Fairchild Semiconductor Research and Development Laboratories for providing some of the devices studied and preprints of their relevant papers. Furthermore, thanks go to Dr. F. Raichlen and Mr. J. K. Okoye for equipment and assistance in digital recording and to Paula Samazan for support in reference work. Karen Current was the patient and excellent typist. Navy contract N60530-68-C-0532 provided funds for computing time, and Tektronix Foundation Fellowships and Teaching Assistantships supplied tuition and expenses for the academic years 1967 through 1970.

ABSTRACT

Burst noise is a normally undesirable phenomenon occasionally found in bipolar semiconductors and other current carrying devices. It is an electrical fluctuation which exhibits itself as one or more rectangular waveforms possessing constant amplitude but random pulse duration. The experimental portion of this study relates only to burst noise in bipolar transistors and operational amplifiers.

Burst noise is not Gaussian as are the more common fluctuations in semiconductors. That fact was established by estimation of the amplitude distribution, a technique found to be sensitive in the detection of burst noise obscured by quantities of conventional noise.

The amplitude of burst noise varies with the parameters of base-emitter voltage, temperature, and source resistance. An exponential increase of amplitude with V_{be} and a lack of dependence on collector voltage implied that the noise originates in the base-emitter junction. A noise magnitude linearly proportional to source resistance over several decades leads one to infer the equivalent circuit of a current source between base and emitter. Current amplitudes of 10^{-10} to nearly 10^{-6} ampere p-p were observed.

Burst noise pulse durations were found as brief as 10 μsec and as long as some 29 hours; neither an upper nor a lower bound was established. The two noise states (high and low, in the rectangular waveform) were treated separately in the duration experiments. Careful measurements on the relative frequency with which the pulse occurred gave duration probability densities of $\frac{1}{\tau} e^{-\frac{t}{\tau}}$ for each state.

That density also applies to a single particle alternately being trapped and escaping and is consistent with the physical theory due to Mead and Whittier relating burst noise to trapping phenomena. Measurements on noise pulse durations in both states as a function of V_{be} lent support to the theory and indicated both trapping and recombination-generation centers were present in samples examined. Another theory, due to Leonard and Jaskolsky, was found inconsistent with the evidence for burst noise's origin in the base-emitter junction. Duration versus temperature dependence indicated activation energies of roughly .5 eV.

Although suggestions in the literature for the power spectrum of burst noise have been inconsistent, digital spectral estimation and judicious use of a wave analyzer showed the spectrum to be flat at low frequencies and to fall as $1/f^2$ at higher ones. Proceeding only from the measured pulse duration probability density, the power spectrum was deduced on theoretical grounds for the first time. The method entailed the derivation of burst noise's autocorrelation function which, when Fourier transformed, yielded

$$S(\omega) = \frac{2}{(\tau_1 + \tau_0)[(\frac{1}{\tau_1} + \frac{1}{\tau_0})^2 + \omega^2]}$$

where τ_1 and τ_0 are the average durations in the two noise states. The expression proved consistent with experiment.

TABLE OF CONTENTS

Chapter I

INTRODUCTION

Burst noise, also known as popcorn noise and bistable noise, is not new to the literature, but it has been inadequately characterized and studied. As an initial working definition, let us term the phenomenon to be a normally undesirable electrical fluctuation abruptly switching between two discrete levels at random times. This phenomenon is observed occasionally in bipolar semiconductor device and elsewhere.

Apparently the first clear reference to burst noise in semiconductors is in a 1956 thesis by R. G. Pay at the University of Birmingham, which work is cited by Bell (1). Pay was studying current spikes in germanium point-contact diodes. It is quite likely that the phenomenon was observed prior to that time and gave rise to numerous explanations such as spontaneous local fluctuations in conductivity or temperature, e.g. as discussed by Van der Ziel (2) in 1950. The first widely published usage of the term "burst noise" is due to Bell (1) in 1960. The origin of "popcorn noise" is traceable to a somewhat apocryphal story of the middle 1960's: the Zenith Corporation was observing a spurious noise in integrated circuits for hearing aids which, when audible, was similar to the sound of popcorn being popped. In fact, it was the linear integrated circuit and its fairly common propensity for burst noise that created the initial interest in the phenomenon. When monolithic operational amplifiers became popular for analog circuit design and attendant difficulties such as burst noise were more widely

known, the industrial magazines devoted much space to the problem. Such interest was summarized by one magazine, EEE (3): "Popcorn noise is a somewhat mysterious stepped-noise phenomenon exhibited by some monolithic op amps at low frequencies. It received considerable attention during the 1968 Linear IC Clinic conducted by EEE but in the 1969 session it was dismissed as under control in newer IC op amps and of no significance in most applications."

The effort described herein is partly experimental and partly theoretical. In the experimental sections, the observations described were made on bipolar devices: NPN transistors and linear integrated circuits. The first such section will give a superficial list of properties characteristic of burst noise, illustrated with typical waveforms. The second section is devoted to the empirical electrical properties. The third chapter covers the time domain characteristics and discusses the time constants associated with burst noise. Chapter Four relates experimental results to a theory propounded by other workers regarding the physical origin of the phenomenon. The next chapter enumerates the measured frequency domain properties of the noise and explains the methods used. The final section of text predicts the power spectral density of burst noise, proceeding only from the statistical model suggested earlier.

Chapter II

THE SALIENT FEATURES OF BURST NOISE

Being an observable physical phenomenon, burst noise is most readily discussed by beginning with the features that are first obvious to the experimenter. Without dwelling on the details of the circuits or the manner of recording, let us examine the fluctuations in output voltage of several devices.

The most commonly found noise waveform is exemplified in Figure 1. The signal is representative of that normally produced by any voltage amplifier and here is generated by a monolithic operational amplifier. The unit was selected because its narrowband noise at 10 Hz is only barely greater than that at 1 kHz (i.e. minimal 1/f noise) and there is no reason to suspect it is other than Gaussian. Figure 2 is the greatly amplified voltage produced by a selected transistor in a grounded emitter configuration. The obvious feature is that the noise signal has discontinuities in level. Therefore the amplitude probability distribution (experimentally, the average amount of time the noise spends at each voltage level plotted versus the voltage levels) cannot be Gaussian but rather appears as if it were bimodal. This figure represents one of the best examples of burst noise seen by this writer. As is typical among the numerous examined devices which exhibit burst noise, there is, in addition to the phenomenon being studied, other noise, presumably Gaussian. Devices have been found which possess burst noise virtually obscured by the remaining variety, in addition to a number of other

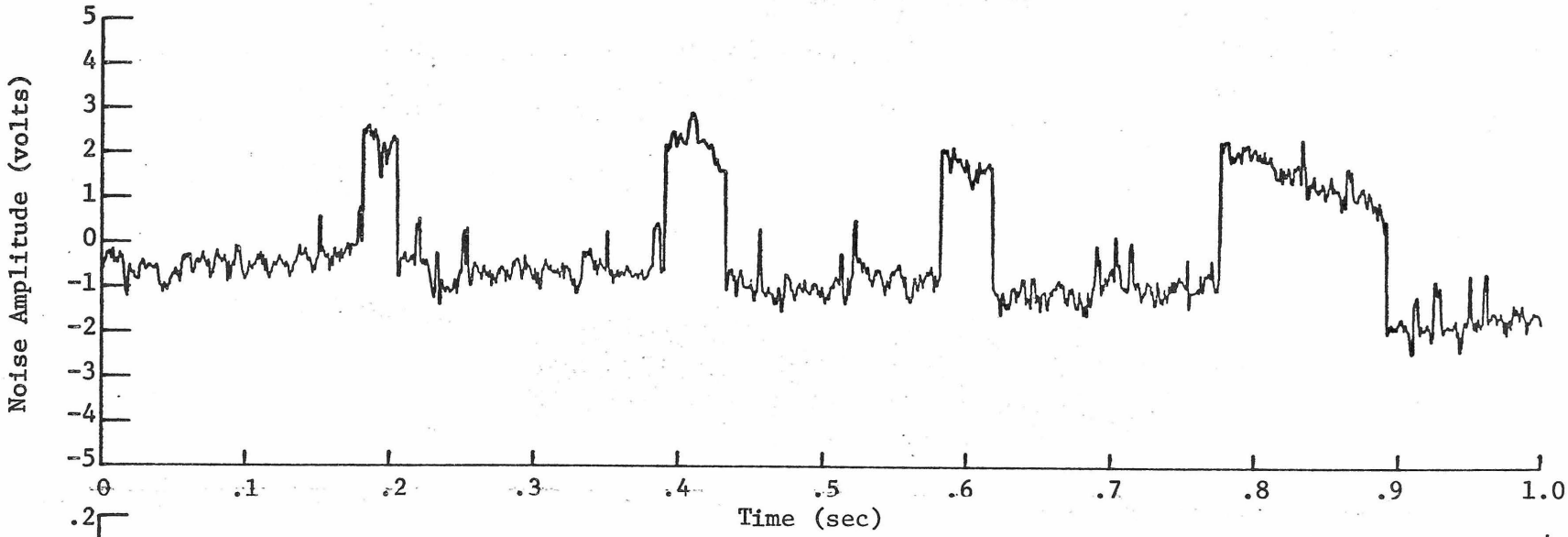

Figure 2

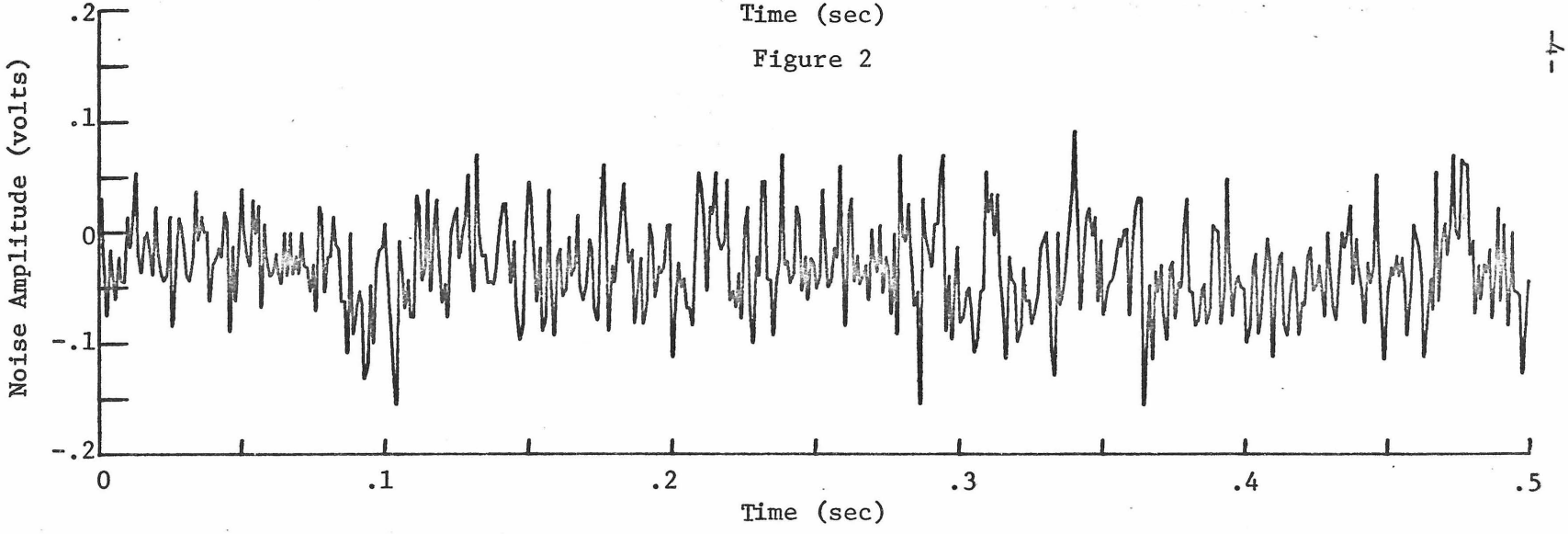

Figure 1

devices in which the burst noise is the predominant effect by a significant margin.

In examining Figure 2, one can conclude several things. There appears to be a constant height rectangular waveform additively superimposed on the more conventional noise that one expects in a transistor. However, we also identify numerous positive spikes about one volt in amplitude in the graph. It is certain from observing a longer record of the source that they are due to another burst noise mechanism in the same transistor since the magnitudes are constant and the spikes are unidirectional as with the larger burst noise pulses. The illustration is perhaps misleading in that the great discontinuities occur at roughly the same intervals. Such is not the case. The temporal distribution will be elaborated upon later, and it is sufficient to note here that examining a longer record leads one to feel the abrupt changes occur randomly in time. Therefore we conclude that burst noise is a rectangular (constant amplitude) waveshape which can occur multiply and in conjunction with the more commonplace device noise.

One may be tempted at this point to compare the classic random telegraph wave of communication theory to an ideal source of burst noise, free of other noise varieties. The telegraph wave makes excursions between two voltage levels at random times but with a constant average number of changes per unit time. The attraction of this comparison is in the familiarity with the statistics and spectrum of the telegraph wave. There is one obvious limitation to this tack in that the telegraph wave has precisely a 50% average duty cycle. Consequently the comparison must be examined in greater detail. This will be done in a later section

with useful results. Among the numerous devices treated in this study, only one exhibited burst noise which in any sense resembled the random telegraph wave in spending roughly half the time in the positive state and half in the negative. The majority of the sources demonstrate pulses which are narrow as the noise apparently favors one voltage level over the other.

The next three plots give some indication as to the varying character of the burst noise which has been encountered. Figure 3 represents a monolithic operational amplifier having several burst noise mechanisms operating simultaneously in sufficient magnitude to obscure the conventional noise. There are three readily identifiable burst noise waveforms superposed here, and there may possibly be more not visible due to their small size. Among the approximately thirty devices of various types found to have burst noise, the norm was the exhibition of more than one mechanism, though patience was often required to identify the second or additional ones.

The operational amplifier of Figure 4 has great, narrow spikes in addition to normal noise. This is one of the rare devices having only a single burst noise mechanism, and it is of interest to examine the pulses' amplitudes and to conclude they are uniform within the measurement accuracy. The difficulty is obviously in determining the actual positions of the baseline and peaks because of the remaining noise. Figure 5 is similar to some of the others, but the source shows two diverse mechanisms: narrow spikes and rare pulses of greater duration.

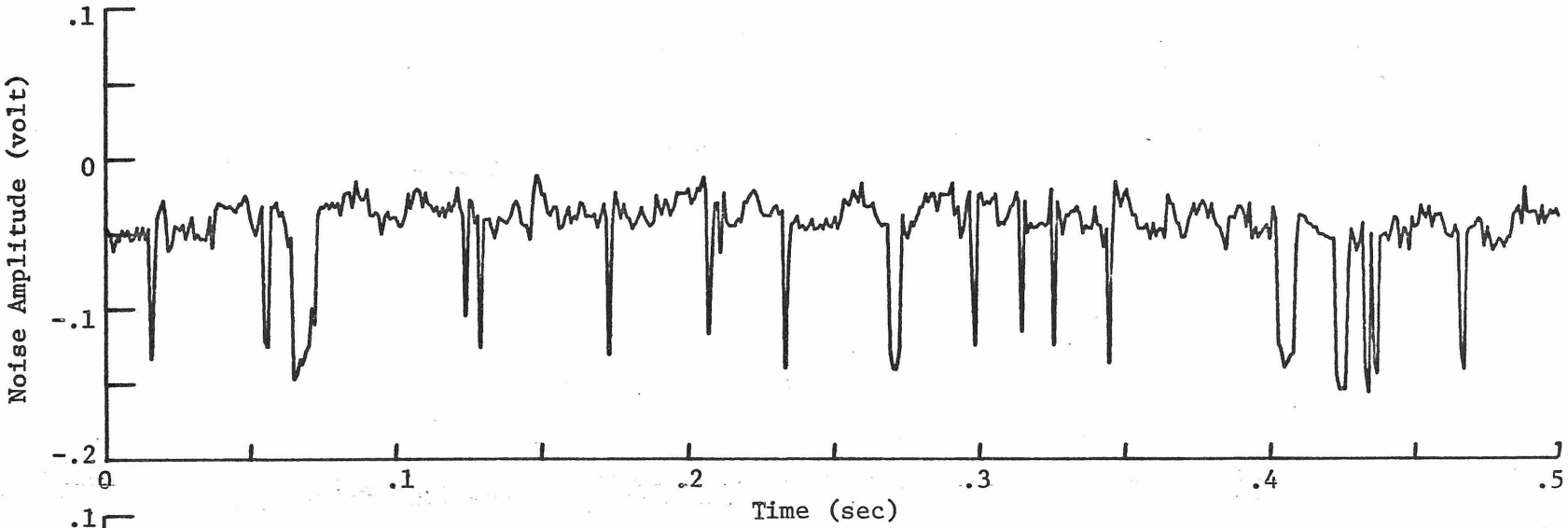

Figure 4

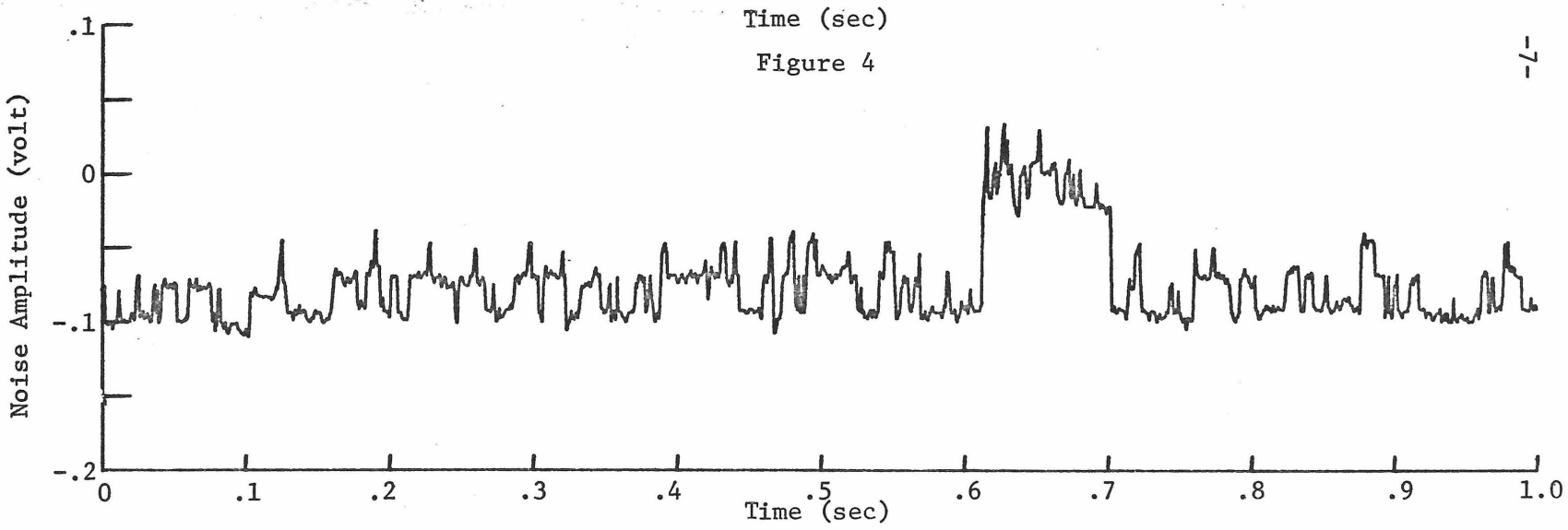

Figure 3

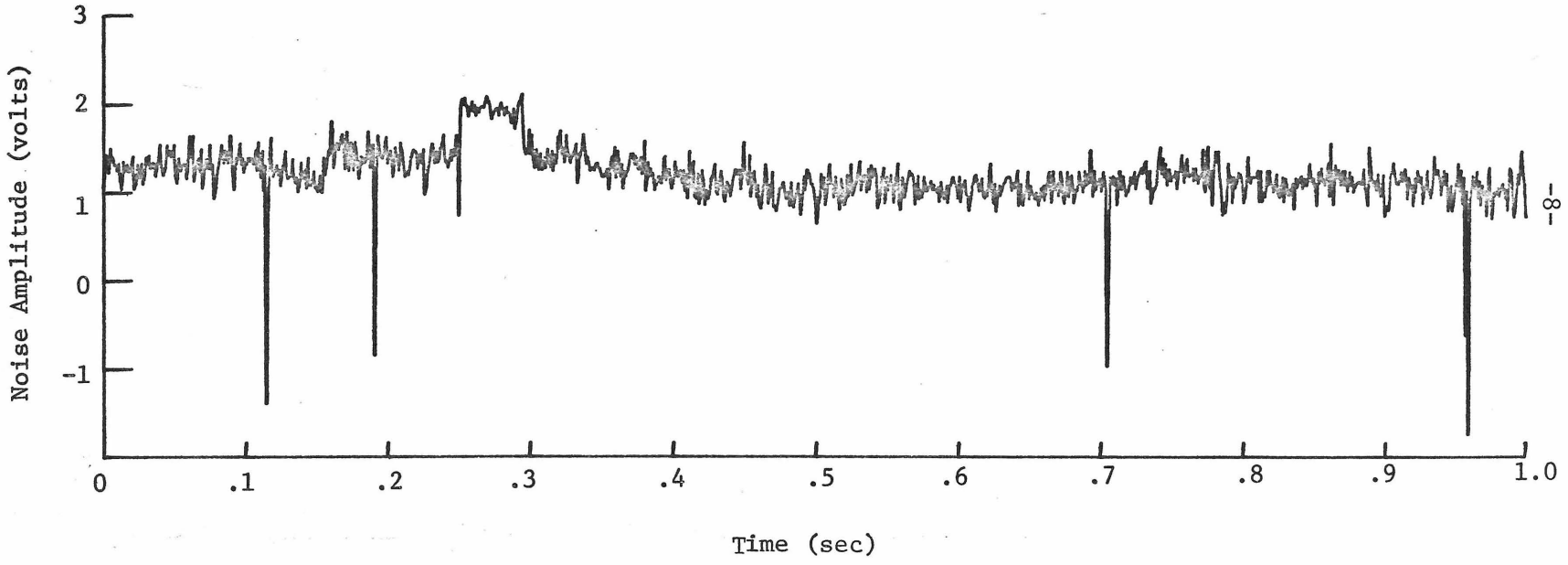

Figure 5

Two additional facts should be brought to fore in concluding the section on burst noise's general features. First, let it be mentioned that burst noise occurs in devices other than bipolar transistors and operational amplifiers. As indicated in the introduction, Bell (1) listed reverse-biased point contact diodes as a source. More recently, those investigations were carried on by Wolf and Holler (4) and by Card and Chaudhari (5). The former group used germanium transistors as diodes; the latter worked with germanium, silicon, and GaSb diodes. Hsu and Whittier (6) have studied the noise in forward biased silicon planar diodes and Schottky diodes. A related discovery was made by Bean, which is disclosed in his paper on discrete conductance fluctuations in artificially prepared protein membranes (7). This work in so-called lipid bilayers has attracted much attention among biologists and should be of interest to those of other disciplines; no attempt to connect the phenomenon to burst noise has been made to date.

Card and Chaudhari also mentioned the existence of burst noise in current carrying carbon resistors. This investigator also observed that noise in attempting to create a 1/f noise source. However, there was difficulty in studying resistor burst noise due to great instabilities. Once a burst noise mode was identified, its existence was too short for meaningful measurement.

The second relevant item is the bandwidth of the system when attempting to observe burst noise, for example with an oscilloscope. Especially when employing operational amplifiers, it is vital to restrict the bandwidth in certain cases so that the wideband, high frequency noise does not obscure the desired fluctuation. In several

instances when μa725 monolithic amplifiers were connected to yield the proper gain, the bandwidth was as wide as 50 kHz, and nothing but the high frequency noise was visible. Using a single R-C pole at 1500 Hz, for example, dramatically unveiled the burst noise present.

Chapter III

BURST NOISE ELECTRICAL CHARACTERIZATION

The present section is devoted to the description of the several properties that are electrically and externally measurable on a bipolar device possessing burst noise and to some implications of the properties. Electrical measurements should be differentiated from temporal and frequency measurements, which will be covered in subsequent chapters.

One obvious characteristic that is simply enough measured is the p-p voltage of a burst noise waveform. Therefore this quantity was examined as a function of device and circuit parameters. A transistor exhibiting one predominant mode of burst noise was connected as a grounded emitter amplifier having its output further increased by an operational amplifier and then displayed on an oscilloscope. In this manner, one can estimate the amplitude of the burst noise within the limits imposed by the obscuring effects of the remaining noise and by the operational requirements of the transistor.

Initially, collector current was taken as the variable parameter, and the input referred noise was found to increase with it in a monotonic but nonlinear manner. The transistor current gain varies with collector current especially at the relatively low currents involved. Therefore the noise measurements were normalized for these h_{fe} changes. As a result, the noise amplitude appeared linearly proportional to the collector current. This simple finding immediately indicates that burst

noise probably manifests itself as base current fluctuations. Figure 6 illustrates the linear dependence of the normalized burst noise amplitude on collector current. The slope is very nearly one on this double logarithmic graph. Because the collector current and base-emitter voltage are exponentially related in a transistor, we have also indicated the measured base-emitter drop on a linear abscissa in the diagram. There exists a clear exponential dependence between this potential and the normalized noise amplitude. Interestingly, the slope to the voltage coordinate corresponds to 29 millivolts. This voltage is only 12% higher than the value of .026 volts belonging to kT/q at room temperature. This second simple observation is further evidence that the noise is related to the base-emitter junction.

Proceeding on the evidence that the source of burst noise is in some manner dependent on the base emitter junction, the source resistance presented to the base was varied. The noise amplitude was found to increase with this resistance. Some difficulty was encountered in using a wide range of resistor values which related to keeping the bias conditions constant at the emitter current (40 μa.) required to render the burst noise clearly visible. Consequently a monolithic operational amplifier was tried instead, the feeling being that the required input current (base current) would be much less and the d.c. parameters would remain fairly constant in spite of changes in source resistance. The configuration is illustrated in Figure 7a. Since Q_1 and Q_2 are normally well matched, being on the same silicon chip, the difference in base potentials is virtually zero and remains so as the resistances seen by each base change but remain equal. If a change

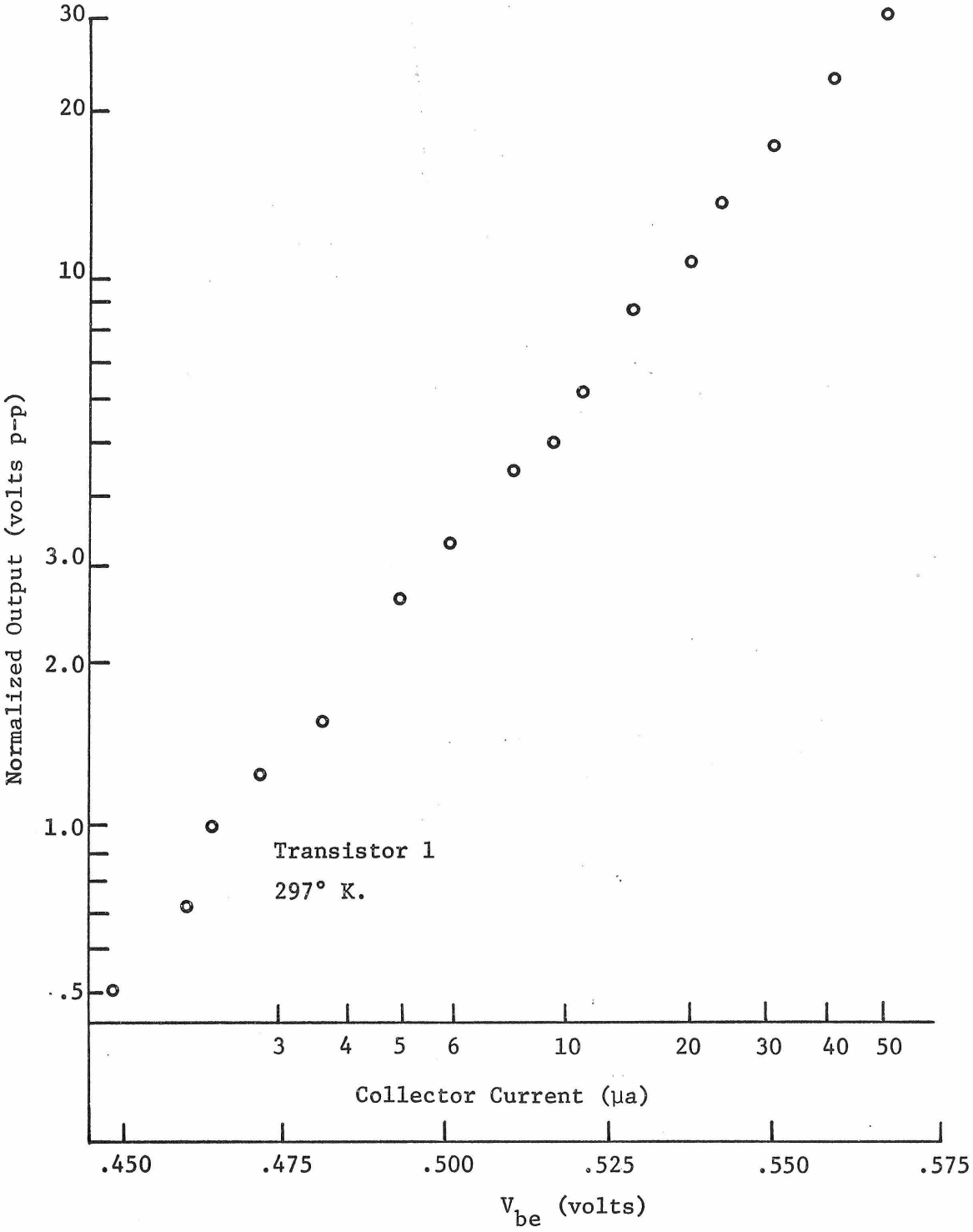

Burst Noise Amplitude Versus Base-Emitter Voltage

Figure 6

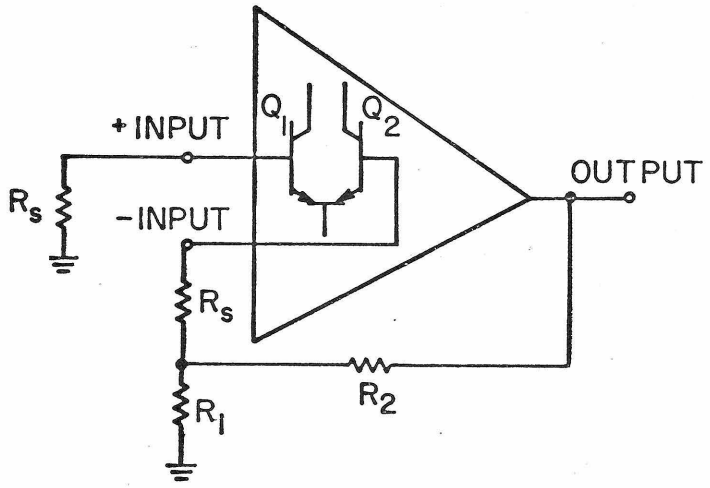

Operational Amplifier Circuit Configuration

Figure 7a.

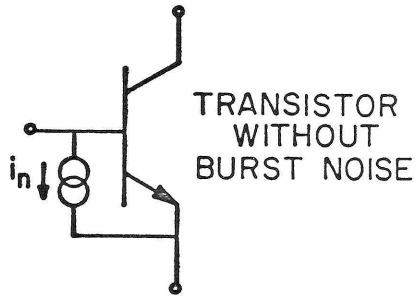

Transistor Burst Noise

Equivalent Circuit

Figure 7b.

in R_s produced a mismatch in base potentials, the unbalance would manifest itself as a change in the output d.c. level. One advantage of the monolithic amplifier is the low bias current required, roughly 10 to 100 nanoamperes, ensuring the constancy of d.c. operating point as R_s is increased. It was found that the source of burst noise in the device used was Q_1 in the particular device examined. That conclusion was based on the reduction in noise amplitude by shunting R_s in the non-inverting input with a capacitor and on the lack of change when shunting the other R_s. Figure 8 gives a plot of the burst noise amplitude versus R_s over some three decades of resistance. Above 1000 ohms the dependence is linear, that is, the burst noise seems to originate as a current source at the base of Q_1 and the burst noise voltage at that point is a function of resistance only. One surmises that the leveling off of the noise level below 1000 ohms results from resistances intrinsic to the two transistors, such as emitter diode resistance and base resistance ($R_{bb'}$), which would place a lower limit on the resistance seen by the current source noise generator. In fact, the resistance may be calculated to be about 1500 ohms for the case of shorted inputs and an emitter current of 10μa. We may conclude that the simple equivalent circuit of a burst noise free transistor with a burst noise current source from base to emitter, as in Figure 7b, should serve as a suitable circuit model. This model is a special case of a general noisy two part model having a shunt current source and a possibly uncorrelated series voltage source, as for example, described by Haus et. al. (8). One should expect then, that the

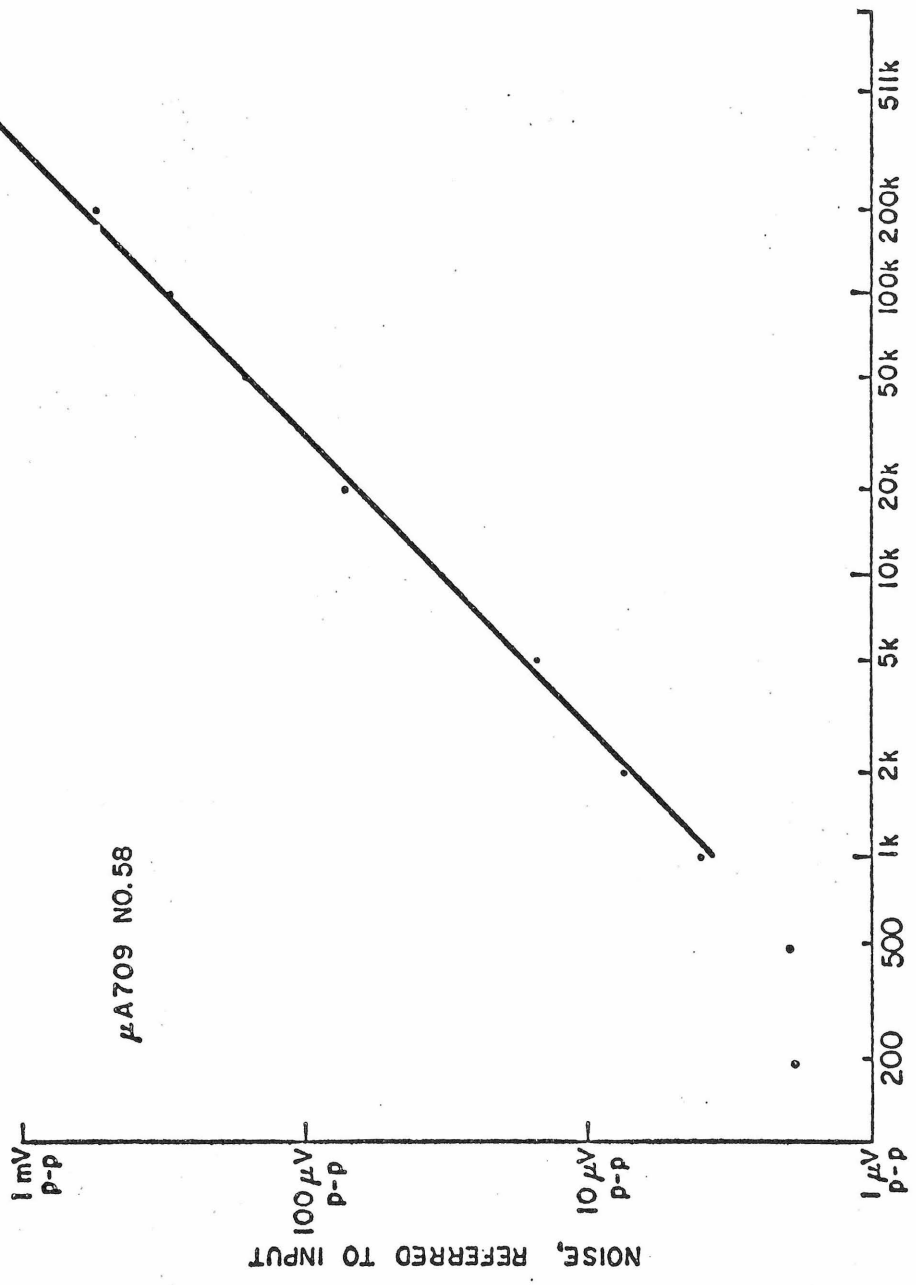

Figure 8. Noise Magnitude Versus Source Resistance

output noise voltage will level off when the source impedance is increased beyond the input impedance of the transistor, h_{ie}. This is, in fact, the case and has been demonstrated with transistors. The levelling off at the high end of the curve does not appear in Figure 8 because of the extremely high input impedance. As a rough but defensible calculation, assume the emitter current is 10μa and the h_{fe} is 200. The differential mode input impedance would be 1.04 megohms, which is larger than the source impedance of .5 megohm.

Having arrived at a sensible electrical model for transistors possessing burst noise, it is rational to speak henceforth of the phenomenon's magnitude exclusively in terms of current. It is well to note at this time that the device in Figure 8 produces a burst noise current of 3×10^{-9} amperes p-p, referred to the input. This experimenter has observed currents ranging from less than 10^{-10} to nearly 10^{-6} amperes p-p in transistors and operational amplifiers.

Another item relevant to this discussion is the behavior of burst noise amplitude with collector to emitter voltage changes. That parameter is somewhat controllable in an operational amplifier having reasonable common mode voltage capability, but utilizing a transistor is more straightforward. Figure 9 gives the burst noise magnitude as a function of collector to emitter voltage for each of two transistors in the configuration of a grounded emitter amplifier. Within the variance of the measurements, the magnitudes remain constant. The observations were performed employing an oscilloscope, which is a powerful technique considering the effectiveness of the human eye and brain in extracting useful amplitude information from a frequently

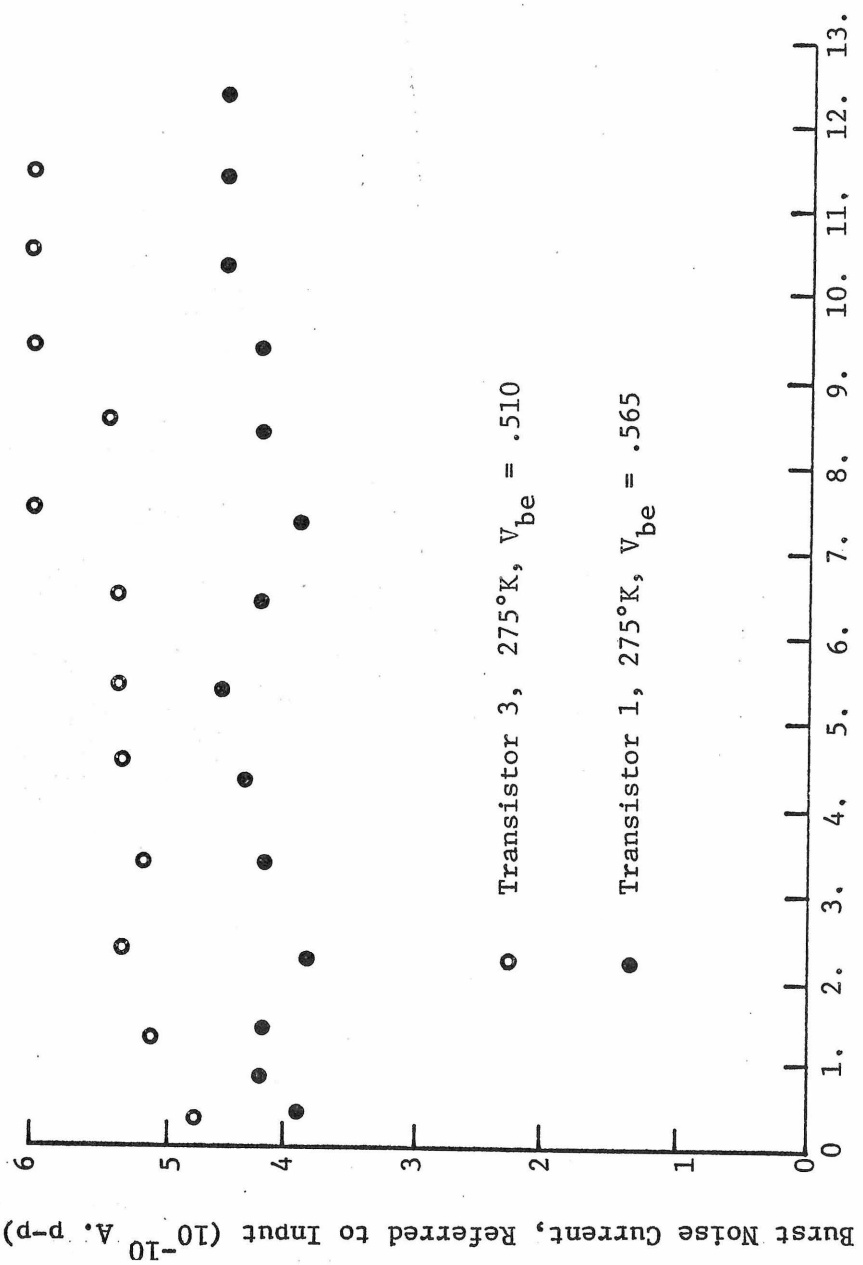

Figure 9. Burst Noise Amplitude Dependence on Collector Voltage

fluctuating waveform. The plotted points vary up to 12% about the mean, which spread is emphasized on the linear plot, but the amplitude appears independent of the collector bias voltage. This observation was reinforced using other devices and other bias conditions. Note that this information is perfectly consonant with the proposal that the origin of burst noise is in the base-emitter junction.

Without pursuing detail, let two additional facts concerning the electrical properties of burst noise be mentioned. First, in attempting to observe any changes in noise character with collector to emitter voltage variations, there was no apparent difference in the typical times between burst noise transitions. Secondly, careful experiments were performed to ascertain the dependence of the average time between transitions on base to emitter bias. The results are covered in detail in Chapter 5, but it is relevant here to mention that in general the average time decreases with increasing base to emitter voltage.

A topic somewhat different from those preceding will conclude the section on the electrical properties of burst noise. We shall be concerned with the probability that the noise voltage is in a certain range of its permissible values. The procedure was to obtain an estimate of the probability density of the voltage, which roughly is a plot of the relative probability of each voltage level versus the voltage. In practice, one makes a histogram demonstrating the relative time the noise signal spends between selected voltage levels, e.g. 0 and .1, .1 and .2 etc. Briefly, the technique was to count the cycles of a 100 kHz oscillator whenever the noise signal was between the

selected limits. By making such a measurement over each voltage range of interest for the same length of time, a histogram may be produced representing the relative percentage of time the signal spends at each level. The details of circuit and experimental configuration are included in Appendix I. The technique of probability density estimation is powerful and sensitive in studying the fundamental properties of noise. Curiously, the process does not appear to have been applied to burst noise before, although it is readily apparent that merely observing waveforms on an oscilloscope is insufficient.

Figures 10 and 11 give the results for the above described procedure using noise produced by two integrated circuits. Ostensibly, one exhibits burst noise, the other does not, on the basis of an oscilloscope examination. The plots are not normalized, but simply present the raw data. Figure 10 appears very much like a Gaussian spread, which should be expected since the origin is in thermal noise and shot noise. In this relatively quiet device, the two noise contributions are roughly comparable. Figure 11, however, corresponds to a bimodal distribution in which there are two ranges of voltage where the signal is quite likely to be found, at about -.9 and +.5 volts. Obviously one peak is favored over the other, which is consistent with the properties of the waveform. The noise appears as a sequence of narrow spikes with an average duty cycle of perhaps 10%, a number roughly corresponding to the relative areas of the peaks in Figure 11. The height of the histogram between peaks is not zero, indicating that finite time is spent there as a result of the system risetime. The peaks have a width of several divisions, resulting from superimposed

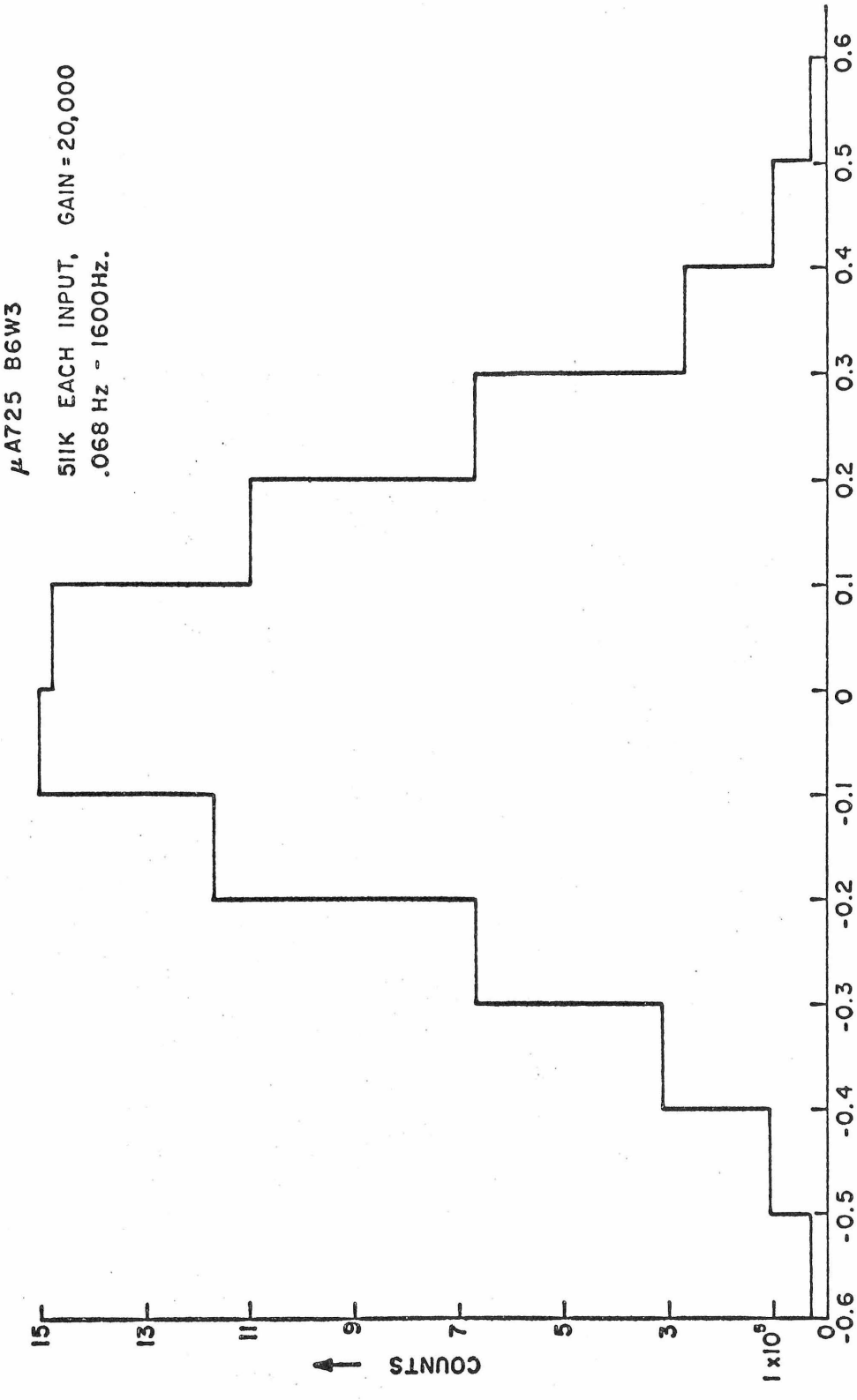

Figure 10. Noise Amplitude Probability Histogram
(Standard deviations smaller than line thickness)

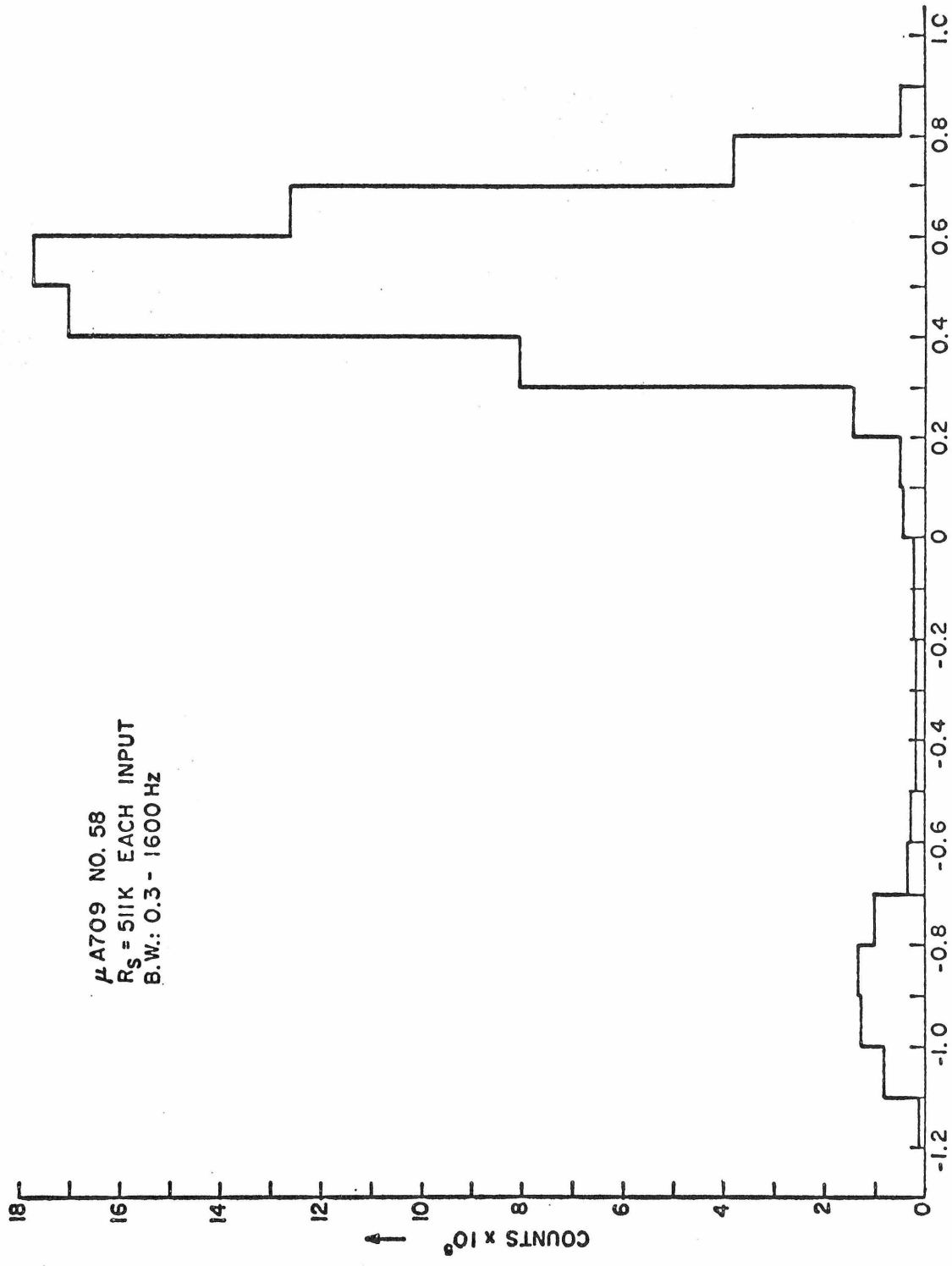

Figure 11. Noise Amplitude Probability Histogram
(Standard deviations smaller than line thickness)

noise which appears approximately Gaussian, although obviously the burst noise itself is not Gaussian.

Figure 12 illustrates the effectiveness of amplitude distribution measurement in discerning the properties of a noise source. Viewing the noise on an oscilloscope yielded no indication of burst noise in this particular integrated circuit. However, in the figure, the presence of a non-Gaussian process is readily apparent, and certain conclusions may be drawn. Presumably the process is burst noise with one level at roughly 0.5 volts on this arbitrary scale, due to the inordinate fraction of time spent there. The large symmetrical region represents the residual Gaussian noise and could well obscure the other burst noise level.

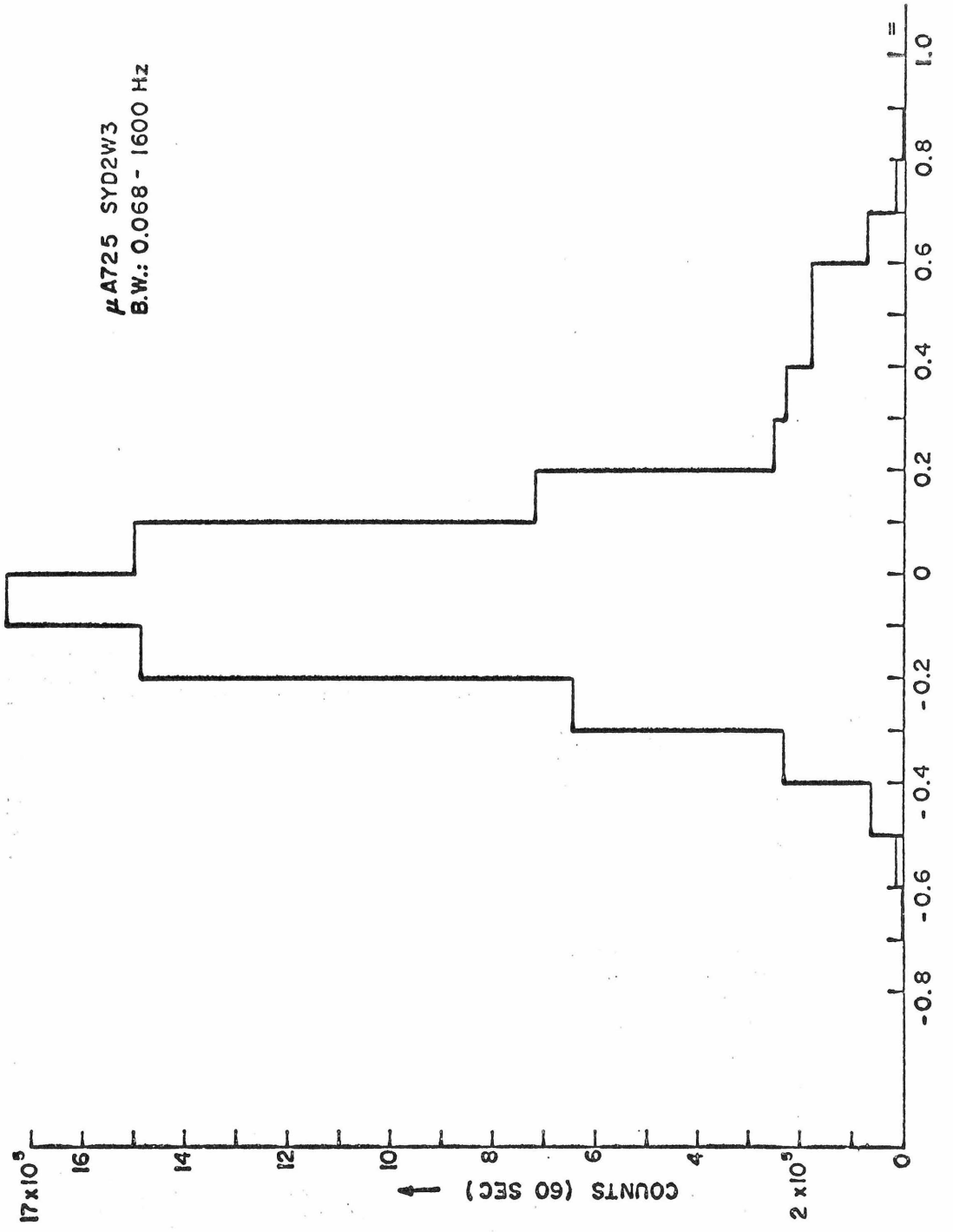

Figure 12. Noise Amplitude Probability Histogram
(Standard deviations smaller than line thickness)

Chapter IV

BURST NOISE TIME DOMAIN CHARACTERIZATION

This section is devoted to a study and description of burst noise considered as a function of time. Idealized burst noise possesses only two discrete voltage levels, assuming the transitions are rapid. Therefore the possible temporal parameters are time between transitions and average frequency, which are interrelated. Figure 13 is a record of ideal burst noise (i.e., free of other fluctuations) showing nine pairs of transitions, although the third and the last are poorly resolved on this scale. For the most part we shall find it useful to adopt the two parameters describing the time between transitions. In Figure 13, the "1" state is the upper level (3.3 volts) and the "0" state is the lower one (-2.5 volts). We define t_1 as any of the times spent in the "1" state between transitions and t_0 similarly for the "0" state. The two parameters are indicated in Figure 13 for two arbitrarily selected times between transitions: one "1" duration and one "0" duration. In the text to follow, "t_1" and "duration in the '1' state" will be used interchangeably as will similar expressions regarding the "0" or low state.

It should be explained that Figure 13 is derived from an actual burst noise source through the use of some relatively straightforward signal processing. Since we seek to study burst noise, it is often desirable to reduce the effects of residual semiconductor noise not useful to us. Therefore for Figure 12 and numerous other

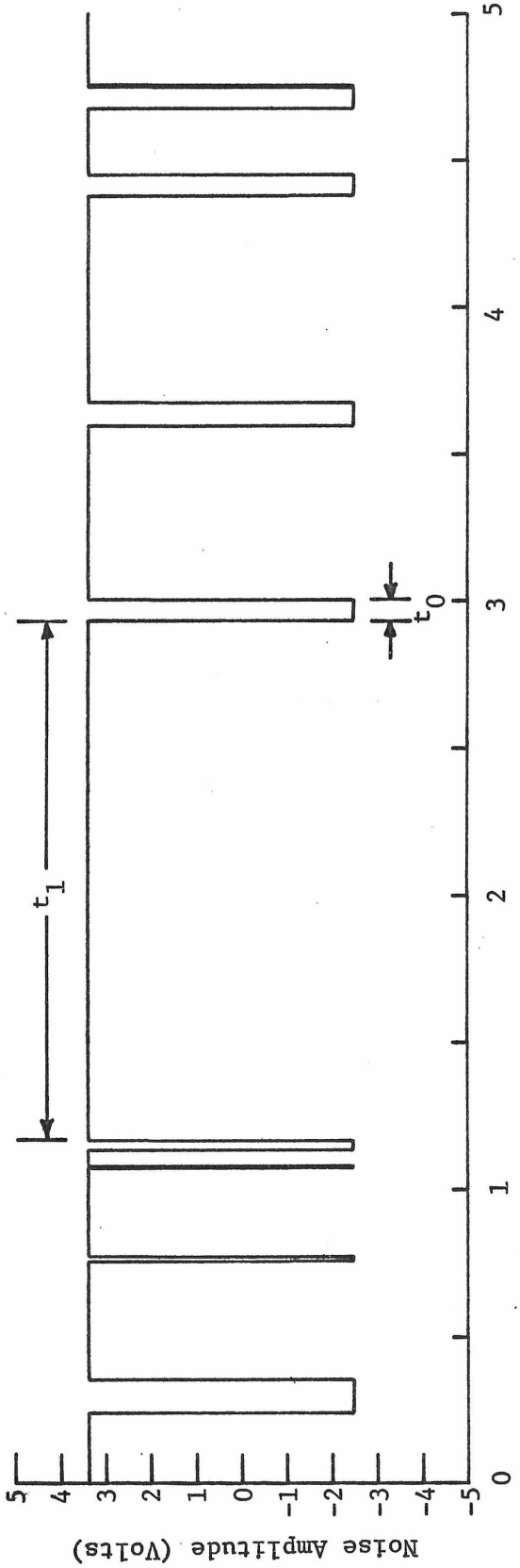

Figure 13

measurements, the noise has been cleaned up to form a purely rectangular wave which is a replica of the original noise source. The circuit for accomplishing this result is covered in Appendix I, and a terse description is included here. The basis for the technique is the use of Schmitt trigger whose hysteretic deadband is smaller than the burst noise amplitude but greater than the remaining noise. The circuit's output state switches when the burst noise changes state but remains undisturbed by other fluctuations, thus producing an approximate copy of the burst noise alone. There are two varieties of error introduced by the Schmitt. First, there is the obvious problem of amplitude: the output voltage excursion is set by the circuit parameters of the Schmitt irrespective of the input noise voltage and is therefore useless for any absolute measurements. Secondly, although the inherent Schmitt delays are only about 50 nsec, there are difficulties in reproducing the timing precisely. If, for example, the burst noise is in transit from low state to high just as the superimposed noise is falling, the Schmitt will switch late. This limitation is intrinsic to the noise source, however, and little can be done to combat it. Fortunately, the estimated errors in the experiments were typically two microseconds (compared with average pulses of the order of .1 to 1 msec). The problem may be aggravated if the burst noise is not large enough to allow a deadband several times the size of the residual noise. However, in the cases of several samples used for measurements, the burst noise was of suitable magnitude. Furthermore, if one is interested in treating average values, presumably the timing errors tend to cancel.

In studying the temporal properties of burst noise, neither

upper nor lower limits have been established for the permissible values of t_1 and t_0. The minimum observable duration in either state apparently is limited by the system bandwidth as might be expected because of the low currents and high impedances involved in amplifiers configured for the observation of burst noise. With the available devices and the utmost care, this experimenter found durations no shorter than approximately 10 μsec. The observed rise-times indicated this period was the limit of system resolution. At the opposite extreme, durations of some hours have been watched. Mr. Michael A. Caloyannides has generously provided a plot (Figure 14) obtained in the course of his 1/f noise studies which is a lengthy record of the noise generated by an operational amplifier. A perfectly clear single burst noise mechanism is evident, though the time scale is appreciably greater than those of other graphs included here. The "1" duration near the beginning of the middle plot is roughly 29 hours.

The first researchers to concern themselves with the duration properties of burst noise pulses were Card and Chaudhari (5) in 1965. They considered only one polarity of pulses in their work with reverse biased diodes and concluded that shorter durations were more frequent than longer ones. They indicated that the rate of occurrence diminished in some exponential fashion with duration, though there could be doubt as to the accuracy of the experiment because of the small number of data points used.

A similar procedure was undertaken, with the following improvements: both polarities of pulses were utilized, up to 30,000 data points were recorded, and transistors were employed rather than

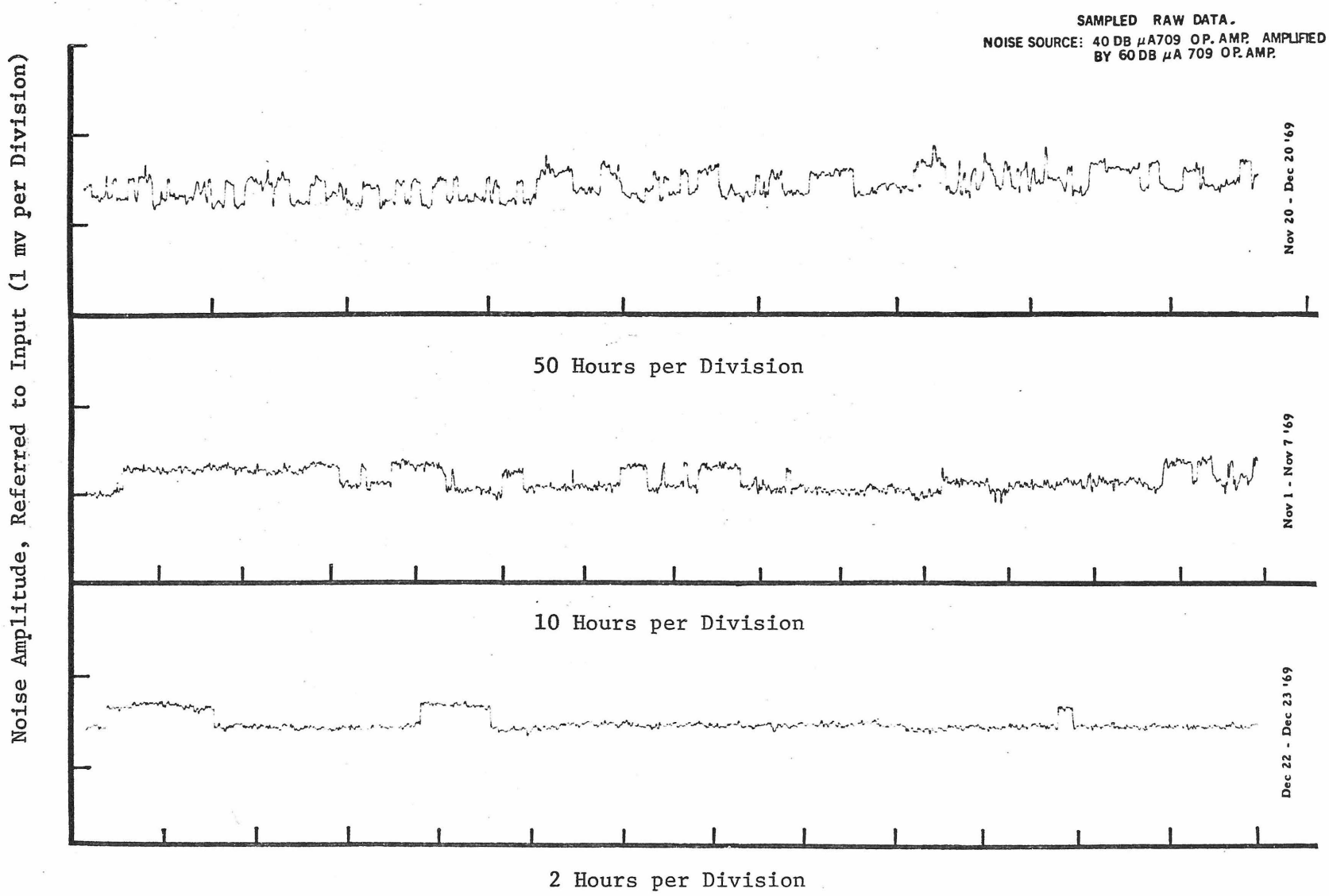

Figure 14. Lengthy Burst Noise Record

diodes. The latter modification is important in that uncertainty regarding the origin and stability of the noise is reduced. Most of the transistors used in this work were fabricated by Fairchild for the explicit purpose of studying the properties and causes of burst noise. The devices possessed the desirable properties of low noise transistors such as constant gain even at low collector current plus the normally undesirable property of exhibiting burst noise. A metal-oxide-semiconductor gate was placed over the edges of the base-emitter junction in each transistor. The noise did not change with several volts of gate bias, which indicated that the burst noise was not a surface effect.

Briefly, the experimental procedure entailed random selection of a noise pulse, measuring its duration with an electronic counter, and recording the result on punched paper tape. The system was automated to take about three points per second, a rate low compared to the burst noise frequencies encountered; therefore adjacent samples are uncorrelated. Each time the system was enabled, the counter would wait until the next noise pulse of proper polarity arrived before beginning its measurement. Thus an unbiased sampling of the pulser was produced. Contrariwise, if a random point on a magnetic tape record of burst noise were selected and the noise pulse overlapping that point were measured, long pulses would be unduly favored over shorter ones.

Sufficiently long records of burst noise durations were made for both "1" and "0" states using several transistors and several temperatures. The durations in each record were ordered and made into a histogram through the use of a digital computer which counted the

number of data falling into 25 μsec wide bins. The resultant plot when normalized gives the probability density associated with any duration in the range covered. Figures 15 and 16 are such plots, showing both t_1 and t_0 densities. The behavior is decidedly exponential, with short pulses the most probable. The histogram increment adjacent to 0 msec is omitted in each case because the system risetime introduces grave error there. Figure 16 is the result of some 30,000 points, nearly a decade greater than the number used in Figure 15. Consequently the statistics are better as shown by the smaller error bars which indicate a standard deviation, the derivation of which is given in Appendix II. The plotted straight line passes through all 3σ regions, strongly indicating an exponential probability density. Such a density is characteristic of a process whose transitions are independent of each other, but the expected number occurring in a given interval is governed by the Poisson distribution. Decaying atomic particles, for example, obey this distribution. If we view trapped charge carriers in a semiconductor junction alternately decaying and "undecaying," then it would be sensible to consider trapping as a candidate for explaining burst noise. In that process, carriers are first mobile, then trapped by a defect of some sort, then mobile again. The period the carrier is fixed and the period the trap is empty have exponential density functions since the process is one of a random walk. These phenomena will be discussed in greater detail in a subsequent section.

Figures 15 and 16 indicate negatively sloping straight lines plotted on semilogarithmic coordinates. Each line represents a functional dependence of the form

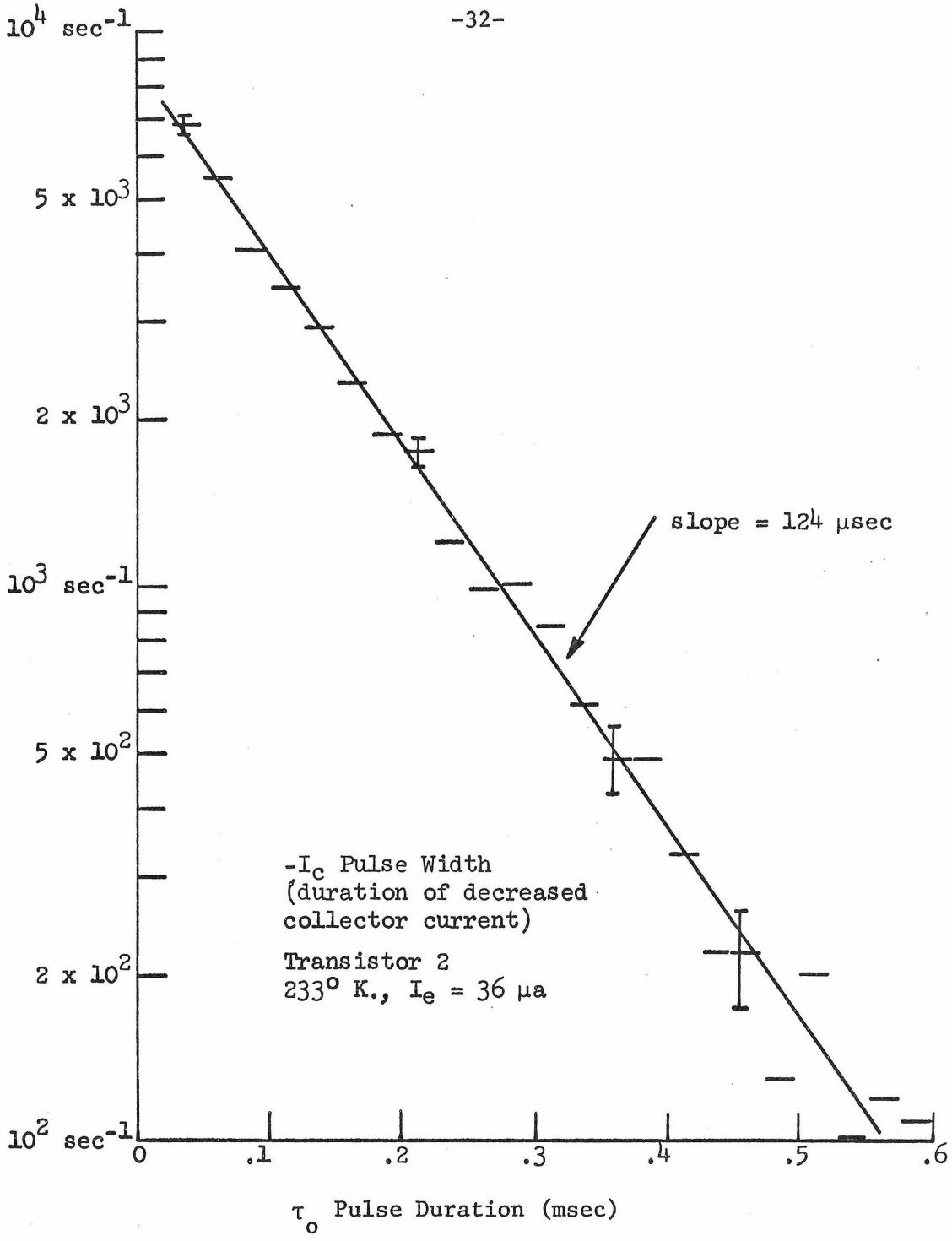

Observed Probability Density of Burst Noise Pulse Width

Figure 15.

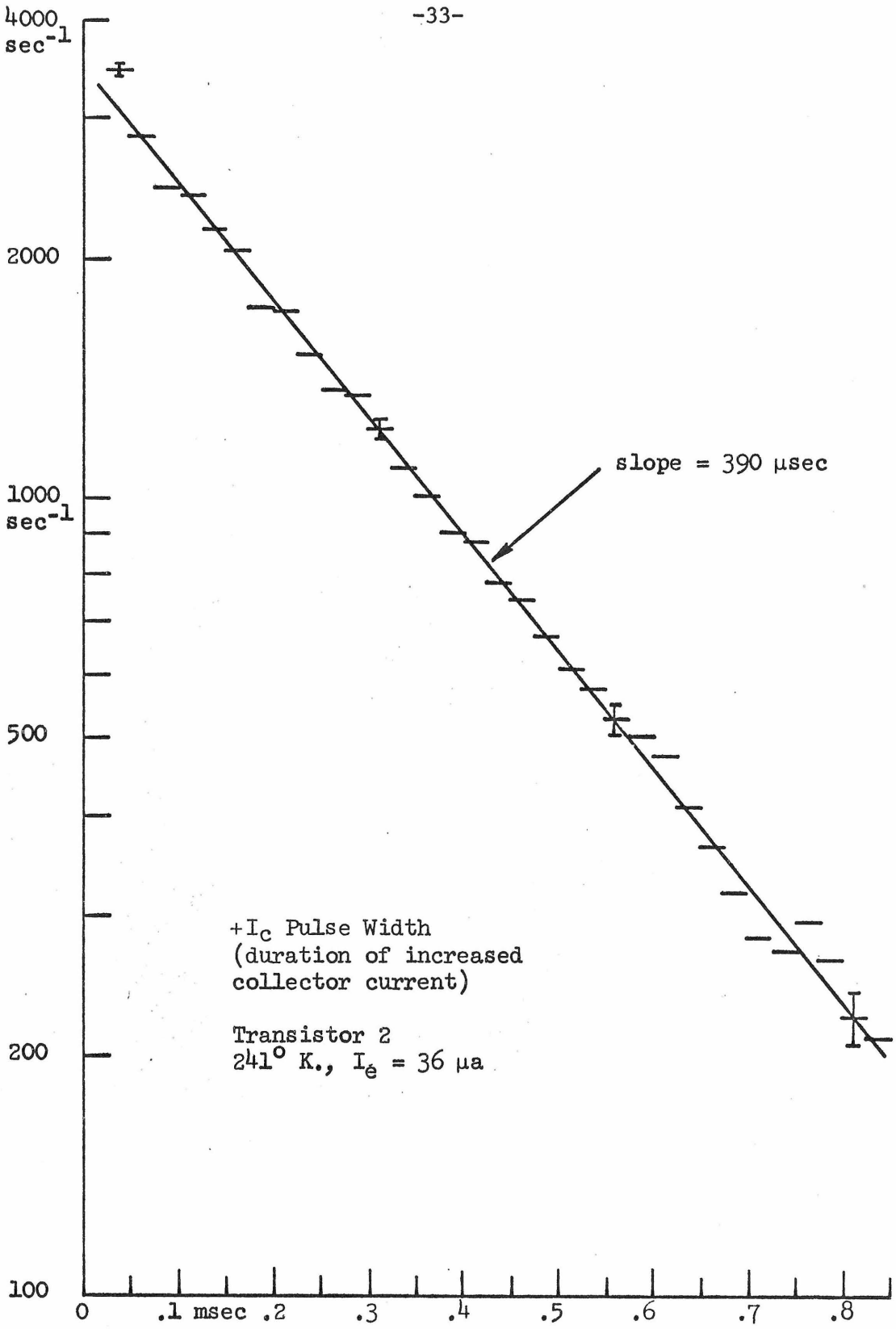
4000 sec^{-1}
2000
1000 sec^{-1}
500
200
100
slope = 390 μsec
+I_c Pulse Width
(duration of increased
collector current)
Transistor 2
241° K., I_e = 36 μa
0
.1 msec
.2
.3
.4
.5
.6
.7
.8
Observed Probability Density of Burst Noise Pulse Width, τ_1

Figure. 16

$$p(t) = Ae^{-\frac{t}{\tau}}$$

where τ is a time constant corresponding to the slope: slope = $-1/\tau$. Recall that the origin of each graph is in the number of pulses of a certain range of durations plotted against the values of the ranges. Since the likelihood of observing a pulse of, for example, .3000 msec is zero, we must actually consider the probability of observing a pulse between (e.g.) .3 and .325 msec long. Therefore $p(t)$ must be a probability density function. The a priori probability that a pulse's duration will lie between T_1 and T_2 (non-negative constants) is equal to time integral of $p(t)$ over the range T_1 to T_2. Since the pulse definitely has a duration, the integral of $p(t)$ over 0 to ∞ is unity, and the constant A must be equal to $1/\tau$:

$$p(t) = \frac{1}{\tau} e^{-\frac{t}{\tau}}$$

Knowing $p(t)$ for the type of random process under scrutiny in this work allows us to compute the most likely average length of pulse we should find by measurement. That is, the expected value of t is:

$$E(t) = \int_{\text{all } t} t\, p(t)\, dt = \int_0^\infty \frac{t}{\tau} e^{-\frac{t}{\tau}} dt = \tau$$

The values of τ in Figures 15 and 16 are estimated to be 124 and 390 μseconds, respectively. One would expect that the average pulse duration would equal the slope in each case. However, the average values seem to be somewhat greater than τ. There are difficulties attendant to

estimating histogram slopes, but probably the greatest bias is introduced into the average by the failure to count short pulses because of equipment risetime limitations. The greatest discrepancy uncovered has been less than 20%. Most are smaller, especially when risetimes (10 μsec) are short compared with the average durations encountered (order of 10^{-3} to 10^{-4} sec). In the next chapter, certain experiments rely on estimating τ by taking averages, and the accompanying accuracy is sufficient for the purpose.

The two values of τ from Figures 15 and 16 apply to the same device under quite similar conditions, one value corresponding to each burst noise state. The fact that the numbers differ is representative of all samples examined. Let the expected values of t_1 and t_0 be represented by τ_1 and τ_0, and consider the implications of differing τ_1 and τ_0 in idealized burst noise. If τ_1 is the greater, more time will be spent in the "1" state than the "0", i.e. the duty cycle $\tau_1/(\tau_1 + \tau_0)$ will be between 50 and 100%. Secondly, the probability of a change of state at any given instant will be one of two constant values, depending on which state the noise is in. Finally, burst noise must be differentiated from the classic random telegraph wave whose duty cycle is 50% and whose probability of transition is constant for every instant.

CHAPTER V

RELATION OF FINDING TO EXISTING PHYSICAL MODELS

The scope of this chapter is not extensive. To date there have been only two physical models proposed for burst noise, and the main thrust of the research here has not been oriented towards the physics. Nevertheless, the origins of the phenomenon are interesting, and their study encourages the consolidation of measurements with theory to provide a more unified concept of burst noise.

The first published transistor burst noise explanation appeared in October, 1969, describing the research of Leonard and Jaskolski (9,10). They contend that burst noise is possible when "an input transistor of the amplifier exhibits a negative resistance region in the reverse-biased collector-base characteristic." (9). Their efforts were concentrated on planar transistors of their own manufacture, many of which had this negative resistance property at collector-base breakdown. The theory was that all anomalous behavior could be traced to miniscule high field regions in the collector-base junction where localized avalanche conditions were occurring. The process in diodes has been described before, e.g. by Haitz et. al. (11) and given the name "microplasma." Leonard and Jaskolski showed that their devices exhibiting negative resistance also emitted light when biased to breakdown, presumably implying microplasma avalanching. Only devices with these latter properties exhibited burst noise when operated under normal conditions, i.e. at lower voltages and higher currents than used in examining breakdown. Evidence was submitted

implying that negative resistance effects were visible on the I-V characteristic, the example being at 25 volts and 70 nanoamperes. The conclusion was that microplasmas are responsible for burst noise.

It is quite possible that Leonard and Jaskolski arrived at an accurate explanation regarding the devices employed, but this writer feels his work and that described in the literature by certain others represent a different albeit superficially similar form of noise. Unfortunately, the two above-mentioned writers devoted comparatively little effort to a study of the noise properties and to how the properties rely on electrical operating parameters. In their work with reverse-biased diodes, Wolf and Holler (4) stated that the burst noise remained unchanged with varying bias voltage until a value near breakdown was reached where another noise, a set of sharp spikes, appeared superimposed on the burst noise. They believed the spikes to be microplasmas. It appears reasonable that Leonard and Jaskolski were indeed concentrating on a study of microplasmas and that their effort was not directed toward the burst noise more commonly encountered.

In defense of this last statement, several items will be proffered. The carefully fabricated Fairchild transistors and several others were found to have no negative resistance tendencies in the base-collector breakdown region but nevertheless possessed burst noise. Furthermore, the noise amplitude is not affected by collector voltage, as indicated in an earlier section. One would expect the mechanism described by Leonard and Jaskolsky to be a function of collector bias, although the evidence they supply is not direct. Furthermore, it is apparent from varying source resistance and base bias that all burst

noise encountered by this worker is associated with the base-emitter junction, whereas the other two contend defensibly that their phenomenon stems from the base-collector junction. In the previous chapter we showed the durations of t_1 and t_0 to be random and to follow an exponential density function. One surmises that a microplasma would not have such a distribution since it is claimed that the length of time it exists is based on thermal considerations. We shall not dismiss the efforts of Leonard and Jaskolsky out of hand, but rather claim they are pursuing a different mechanism.

The majority of this chapter will be devoted to the second theory and some observations which we shall find consistent with it. This theory is due to C. A. Mead of the California Institute of Technology and R. J. Whittier of the Fairchild Semiconductor Corporation. Briefly, the physical model is predicated on the existence of two defects in the transistor's base-emitter junction: a gross metal precipitate and a more minor and common defect, such as impurity adjacent to it. It is also within the scope of the concept that the process could take place at the surface of the semiconductor with a surface trap playing the role of the minor defect. The experiments here were made predominantly in devices having gate electrodes which could be biased to demonstrate that the burst noise was not of surface origin, although surface charges could well be responsible for the noise in other devices. The function of the precipitate is to cause bending of the conduction and valence bands and modulate the flow of current according to the effect of a trapped charge in the minor defect. The region about the precipitate may be viewed as two metal-semiconductor junctions back to back with

energy plots given in Figure 17. Assume for ease of discussion that the minor defect is in the n-type material and that the doping is such that the current flowing under forward bias is controlled to a large extent by the n-semiconductor to metal Schottky barrier height. The presence of an electron in the trap increases the barrier height (and thickness if tunneling is important) as shown in the middle and lower illustrations.

The electrons in the n-region conduction band must surmount the barrier to reach the metal and p-region. Therefore in our simple illustration the base to emitter current will be reduced when an electron is caught and increased during any period when the trap is empty.

Regardless of the actual mechanism responsible, it is reasonable to conclude that a single carrier trapped or emitted controls the noise by virtue of the consistency of the observed noise amplitude and the exponential probability densities of the burst durations. Consequently we must familiarize ourselves with the characteristics of trapping centers. Perhaps the most readable discussion of this topic is in Physics and Technology of Semiconductor Devices by A. S. Grove (12) the following brief discussion is patterned after that work.

There are four independent mechanisms whereby charge can be transferred to or from a trapping center. These four will be denoted by the letters (a) through (d) and are schematically illustrated in Figure 18. Process (a) involves the capture of an electron from the conduction band. (b) is the emission of an electron from the trap to the conduction band. Mechanism (c) consists of the trap capturing a hole from the valence band, which is equivalent to the trap's emitting

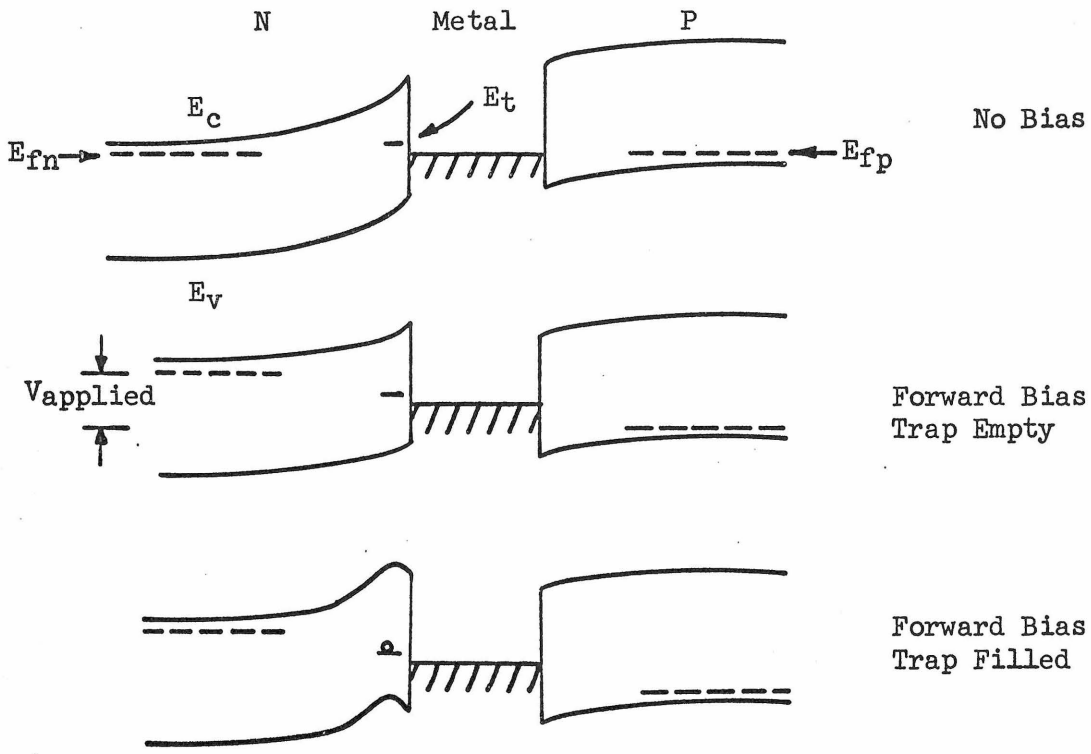

Figure 17

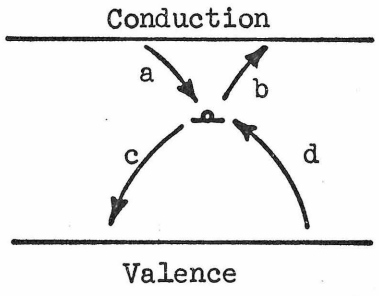

Figure 18

an electron into the valence band. (d) is the emission of a hole by the center to the valence band or the trapping of an electron from the valence band which leaves a hole there. With each of these four mechanisms there is associated a time constant, which is the expected trapping or emission time. It is reasonable that these constants be proportional to the reciprocals of the defect trapping cross section, the electron thermal velocity, and the number of electrons available for trapping or the number of states an emitted electron may occupy, Therefore,

$$r = \frac{1}{\tau} = \sigma \, v_{th} \, N$$

In the above expression r is the rate of emission or trapping, i.e. the reciprocal of the time constant. In the case of process (a), N is the electron concentration $N_c \, e^{(E_{fn} - E_c)/kT}$, where N_c is the effective density of states in the conduction band, E_{fn} is the electron quasi fermi level, and E_c is the conduction level. Situation (b) is similar, again involving the density of states and an exponential probability of emission across a certain energy gap: $N = N_c \, e^{(E_t - E_c)kT}$. E_t is the trap energy level. Expressions for (c) and (d) are like the first two with suitable constants substituted to represent the valence band. The results are summarized below with τ_+ representing the expected time during which the defect is devoid of an electron and τ_- the opposite. It is well to mention here that processes (a) and (c) are dependent on the base-emitter voltage since the difference in quasi fermi levels $E_{fp} - E_{fn}$ equals the potential applied to the junction.

$$\text{(a):}\quad \frac{1}{\tau_+} = r_a = \sigma_n \; v_{th} \; N_c \; e^{\frac{E_{fn} - E_c}{kT}}$$

$$\text{(b):}\quad \frac{1}{\tau_-} = r_b = \sigma_n \; v_{th} \; N_c \; e^{\frac{E_t - E_c}{kT}}$$

$$\text{(c):}\quad \frac{1}{\tau_-} = r_c = \sigma_p \; v_{th} \; N_v \; e^{\frac{E_v - E_{fp}}{kT}}$$

$$\text{(d):}\quad \frac{1}{\tau_+} = r \; = \sigma_p \; v_{th} \; N_v \; e^{\frac{E_v - E_t}{kT}}$$

Certain properties of two transistors exhibiting single, strong burst noise mechanisms have been measured in an effort to identify some characteristics of the trapping centers. The procedure was to determine the average duration of each of the two noise states for variations in temperature and base-emitter voltage. In finding the average duration, the repetition rate was first measured by counting the number of burst noise excursions in 10 one second intervals. To complete the process, the noise was used to gate a 1 MHz signal which, when counted, indicated the duty cycle of the noise, that is, the percentage of time spent in the selected one of the two states. The average duration in either state is simply the proper one of the two duty cycles divided by the average frequency. Appendix I includes the relevant circuit diagrams for the experiment.

Figures 19 and 20 exhibit the dependence of the two burst noise time constants upon V_{be} for two different transistors. The first illustration shows an approximately exponential dependence of both noise states on V_{be}. Processes (a) and (c) are the only two that depend on the fermi levels and therefore both must be involved.

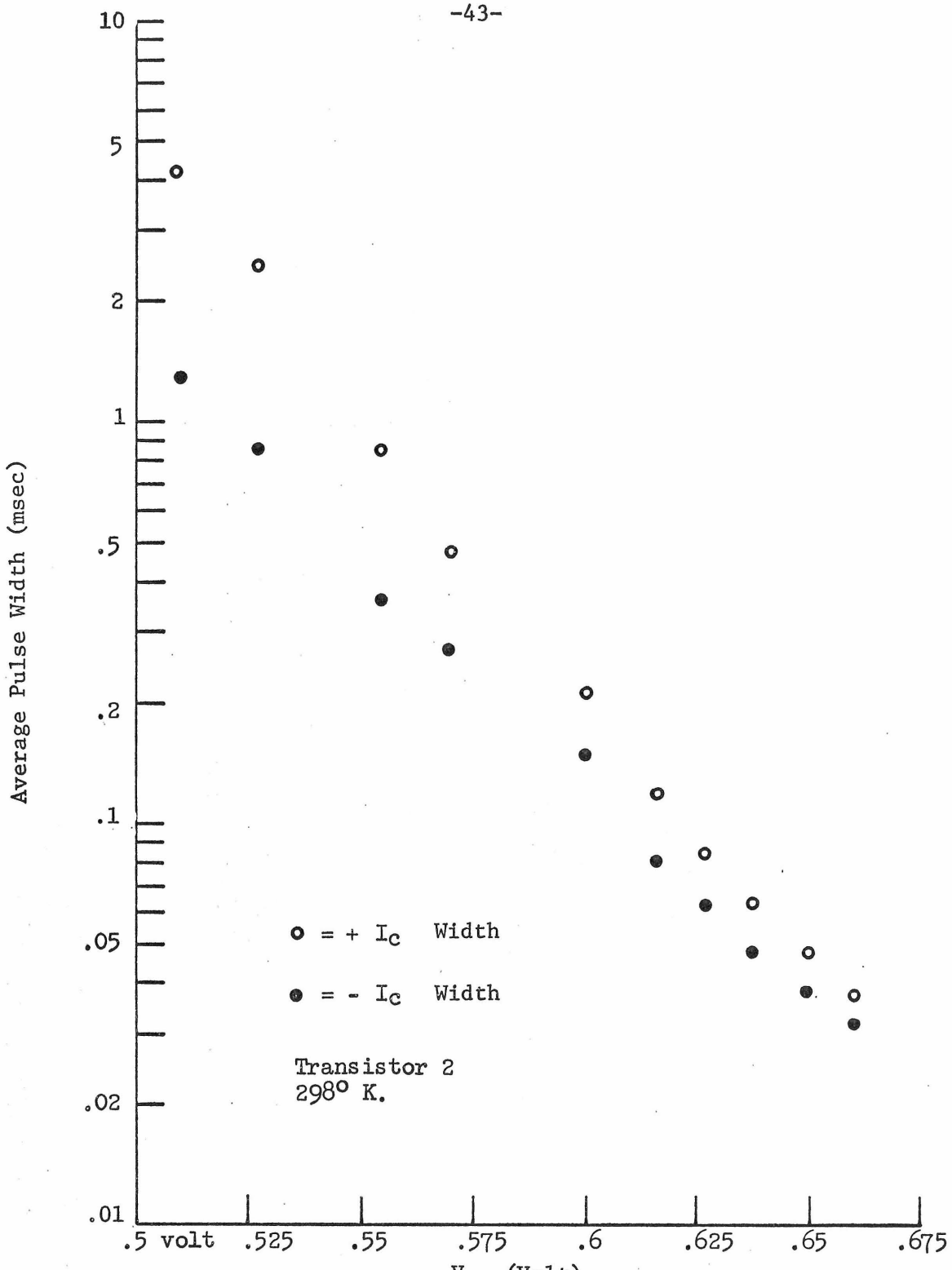

Average Burst Noise Pulse Width Versus Base-Emitter Voltage

Figure 19

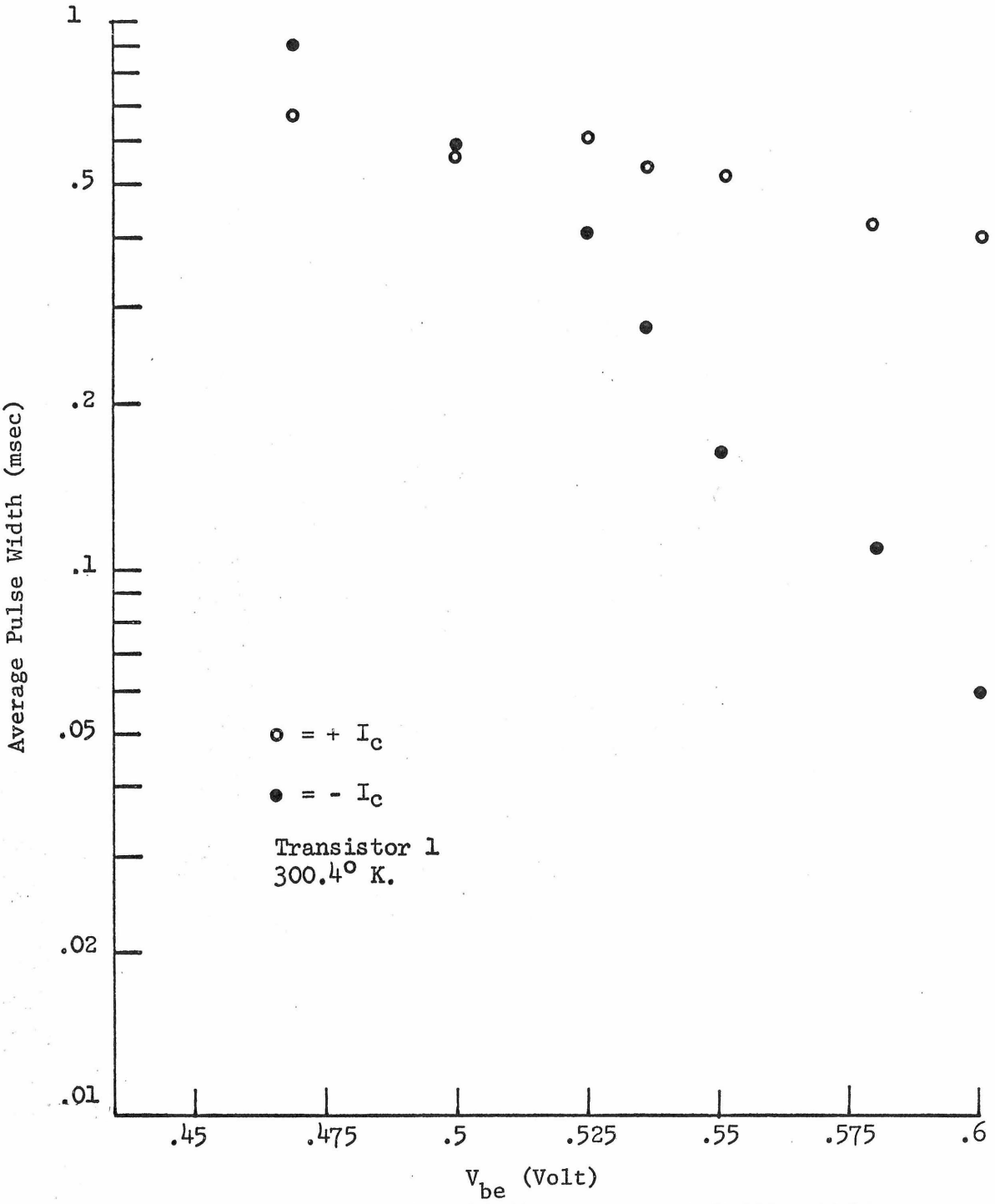

Average Burst Noise Pulse Width Versus Base-Emitter Voltage

Figure 20

Consequently the defect must be functioning as a recombination-generation center. Figure 20 indicates that the state corresponding to decreased collector current is a strong function of V_{be}, but the other state is not. Decreased I_c corresponds to a decrease in base current and to an increase in base-emitter current. The latter implies that the defect is empty of an electron. Since τ_+ having a V_{be} dependence implies process (a), and τ_- having none implies process (b), we are led to conclude that this sample's defect is functioning as a trap. That is, the site's charges communicate only with the conduction band.

Figures 21 and 22 yield energy information relating to the defect centers. The logarithm of average burst duration of both burst noise states is plotted against reciprocal absolute temperature. All four time constant expressions contain an exponent of an energy over kT, therefore the slopes of these plots equal the socalled activation energy, ϕ, divided by Boltzmann's constant. The observed values of .4 or .5 eV are a little less than half the energy gap in silicon. The sample of figure 21 is the one possessing the generation-recombination center, i.e. both time constants are functions of fermi levels which are linear functions of base-emitter voltage. Note that all four lines have an activation energy plus V_{be} of about the same value, a little over a volt. The increased I_c line for the second sample shows that the trap is .44 eV removed from the conduction band.

The information uncovered in the several experiments is seemingly consistent with the trapping theory propounded by Mead and Whittier. The proof described here is of course insufficient for

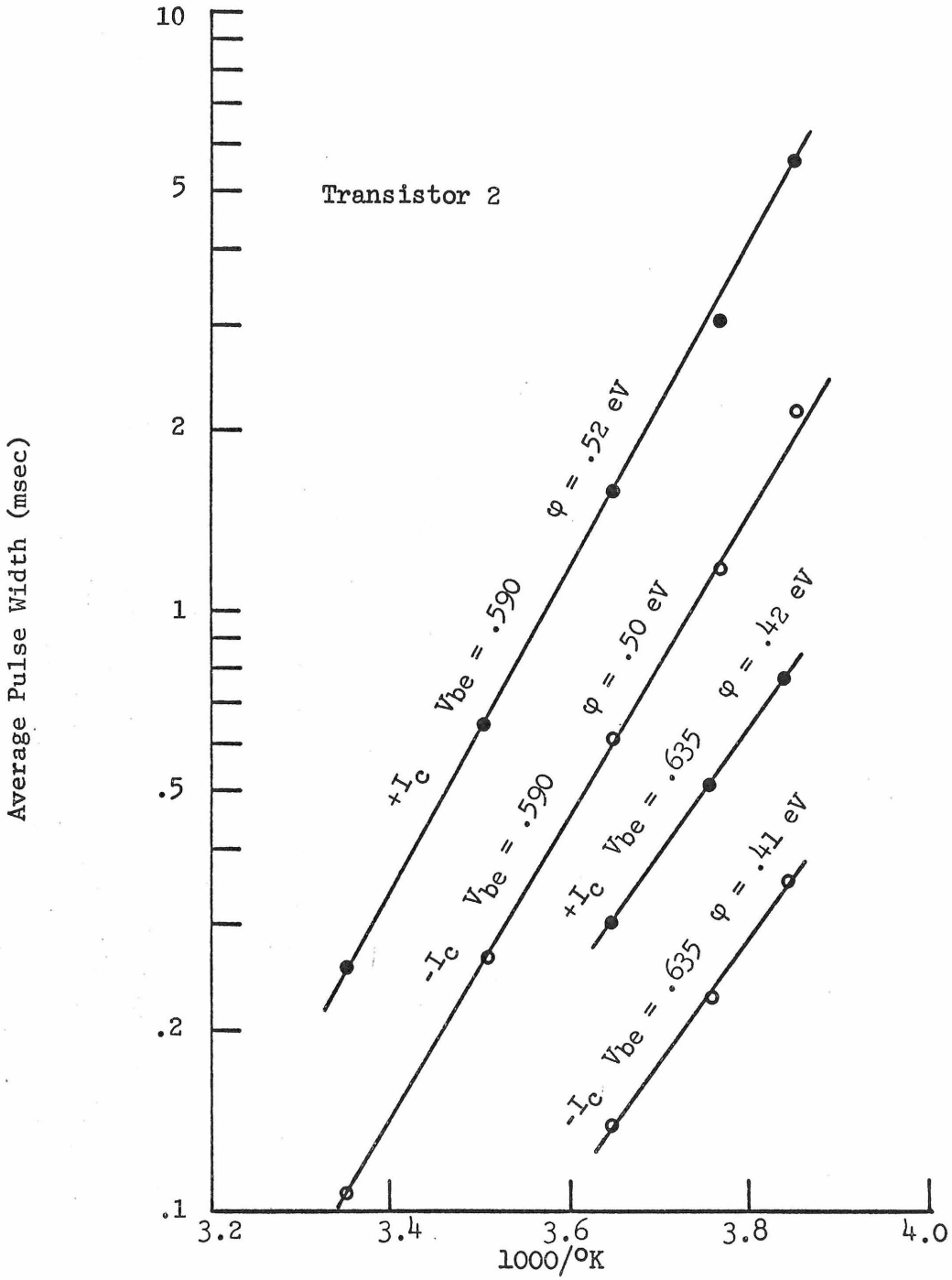

Average Burst Noise Pulse Width Versus Reciprocal Temperature

Figure 21

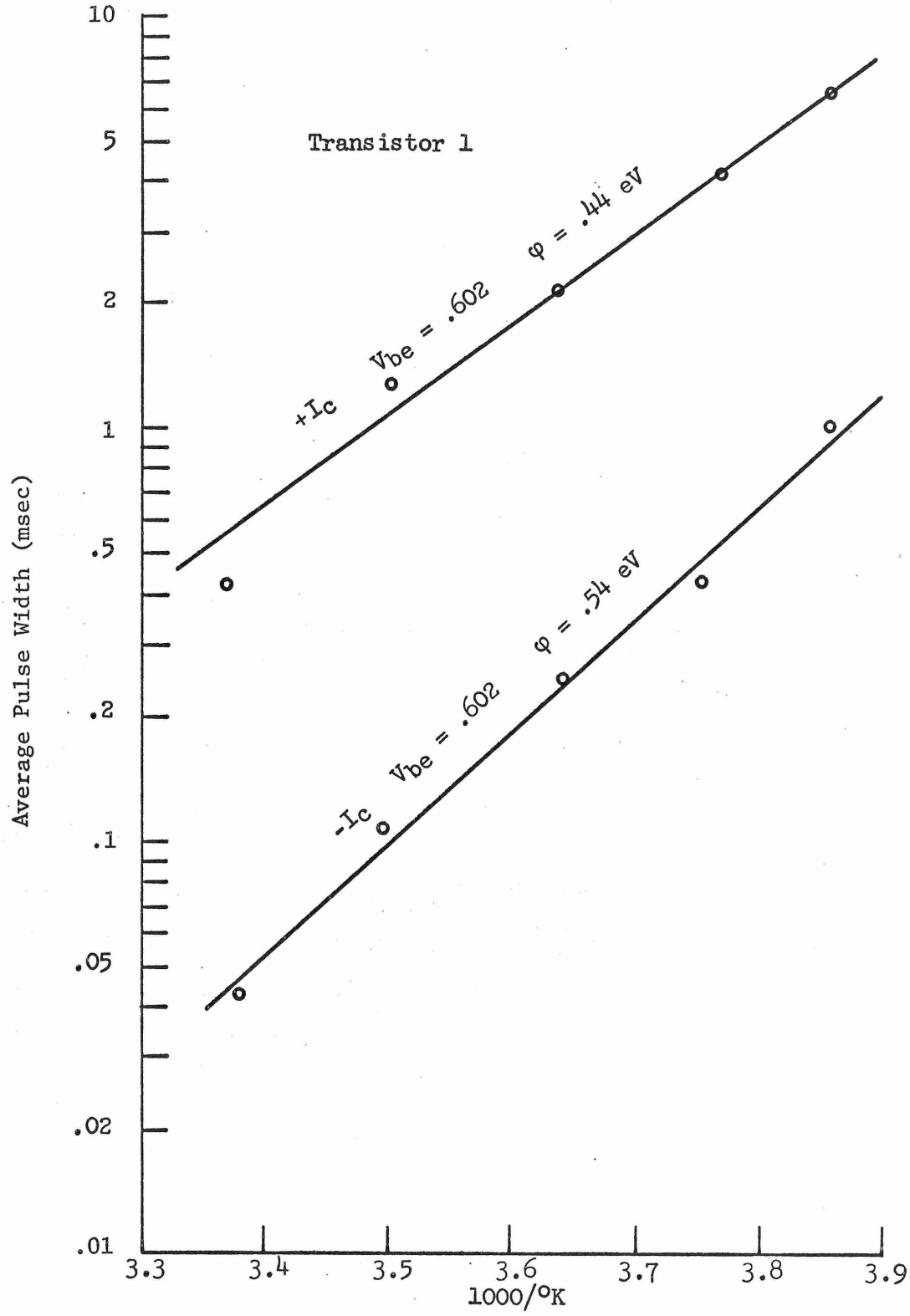

Average Burst Noise Pulse Width Versus Reciprocal Temperature

Figure 22

determining the validity of the trapping argument relying on the existence of a metal precipitate, although evidently burst noise originates in the base-emitter junction and is related to trapping defects. Recently Hsu, Whittier, and Mead (13) disclosed experiments which more accurately tie burst noise to its origins in precipitates.

CHAPTER VI

BURST NOISE FREQUENCY DOMAIN CHARACTERIZATION

The most apparent spectral property of devices having burst noise is the relatively great low frequency spot noise. That is, narrow band noise measurements at 10 Hz, for example, are uniformly greater than at 1000 Hz if burst noise is present. The three integrated circuits employed for the amplitude probability density measurements (Figures 10 - 12) were examined to ascertain the narrowband current noise at four points in the audio spectrum; the results are tabulated below. Units are picoamperes/$\sqrt{\text{Hz}}$, referred to the input.

	10 Hz	100 Hz	1 kHz	10 kHz
Fig. 10	.34	.21	.17	.15
Fig. 11	25.	20.	3.3	.40
Fig. 12	1.34	.39	.26	.20

Recall that Figure 10 represents an apparently Gaussian source, Figure 11 possesses gross burst noise, and Figure 12 has burst noise, albeit virtually obscured by the normal noise. Within a factor of about two, the 10 kHz figures are equal. Dropping in frequency three decades indicates a noise increase of roughly two for the quiet device, an increase of about sixty for the unit with gross burst noise, and perhaps six where there is only a moderate amount of burst noise. The figures are representative of all the devices examined for spot noise current.

Evidently burst noise has a power spectral density which

decreases with increasing frequency. Therefore the relevant question at this juncture relates to the precise functional dependence. The consistent data in the literature are insufficient to give any generally agreed upon form for the power spectrum. Hsu and Whittier indicate findings of $1/f^n$ spectra in transistors and among samples of specially fabricated diodes with gates over the junctions. Spectral plots are shown in their publication (6) having $n \sim 2$ for a diode and $n \sim 1$ for a transistor. In the case of the diode, the slope diminishes locally at 100 Hz but returns to a value of approximately 2 at 10 Hz. Wolf and Holler (4) include a carefully made spectrum plot having a $1/f^2$ character from 10^4 Hz to 10^2 Hz, where it ends and the slope appears to diminish. None of the above researchers pursued the spectrum to frequencies low enough to establish a deviation from the $1/f^n$ character. Card and Chaudhari (5) utilized a sample for which τ_1 was very nearly equal to τ_0 as is the case of the random telegraph wave, whose spectrum is derived, for example, by Papoulis (14). Consequently they predicted a spectral density of the form

$$S(f) = \frac{A}{1 + (f/f_o)^2}$$

and claimed to have measured such a spectrum although no results are actually given. In sum, we haven't a very clear idea of a burst noise spectrum, although the approach of Card and Chaudhari for the specific case of $\tau_1 = \tau_0$ appears reasonable.

An effort was made to perform a more complete estimate of the

burst noise power spectrum of a transistor. To this end, a Hewlett-Packard 302A wave analyzer was employed as a narrowband tuned voltmeter having a 3 db. bandwidth of 7 Hz. The unit is fundamentally intended for sinusoidal distortion measurements, and as a result the ballistics of its meter render it unsuitable for narrow bandwidth noise measurement. Fortunately the instrument has a connector providing the signal output following the narrowband filter. The narrowband signal is then measured by an rms (thermocouple) voltmeter which in turn provides an analog output which we pass through an R-C integrating filter into a high impedance voltmeter. Thus the system functions as a tuned voltmeter with a long averaging time.

The second technique we have readily at our disposal for power spectrum measurement is due to Blackman and Tukey (15). Fundamentally, the method has as its premise that the power spectral density of a random process is simply the Fourier transform of its autocorrelation function. If we are somehow able to estimate the form and magnitude of the latter, we can arrive at useful knowledge regarding the spectrum. Some mathematical details of the procedure are included in Appendix III in addition to a terse but more detailed introduction to the subject. In practice, the noise of interest was sampled, digitized, and recorded on magnetic tape by a Digital Data Systems model 1103 data acquisition system. Using a sufficiently fast sampling rate enables one to submit a record of the noise to a computer and retain sufficient information to produce an estimated autocorrelation function. This function is, naturally, not continuous but digitized, and the Fourier transform of

it is a finite cosine transform. The spectral estimate is produced for each frequency by a weighted average of several cosine transform points. Only the basic steps have been included here; the powers and limitations have not been discussed. However, digital spectral estimation is a powerful tool and of significant value.

The first attempt to obtain a burst noise spectrum by the tuned voltmeter technique is documented in Figure 23. At frequencies higher than 3 kHz, the dependence is $1/f^2$. There is a "knee" at approximately 1 kHz, below which the slope approaches 0.7. The graph has precisely the same shape as the spectral plot included by Hsu and Whittier (6) in their recent description of a burst noise diode. Judging from the upper and lower frequency limits and number of points in their plot, it is extremely likely they also employed a wave analyzer. Unfortunately there is a danger of anomalous readings at low frequencies using this method as the wave analyzer functions on a superhetrodyne principle. The instrument beats the tuned frequency down to d.c., filters with a lowpass network, and beats the result back up to the original frequency. Therefore, there are potential difficulties such as images and oscillator feedthrough at the lowest frequencies. In the initial configuration, furthermore, there may have been a ground loop or similar source of line frequency, for when the experiment of Figure 23 was duplicated to study the low frequency behavior, enough 60 Hz energy was detected to raise significantly the readings at 50 and 70 Hz. There was also some influence at 120 Hz. The proof that the low frequency measurements represented in Figure 23 are high is twofold. First, a

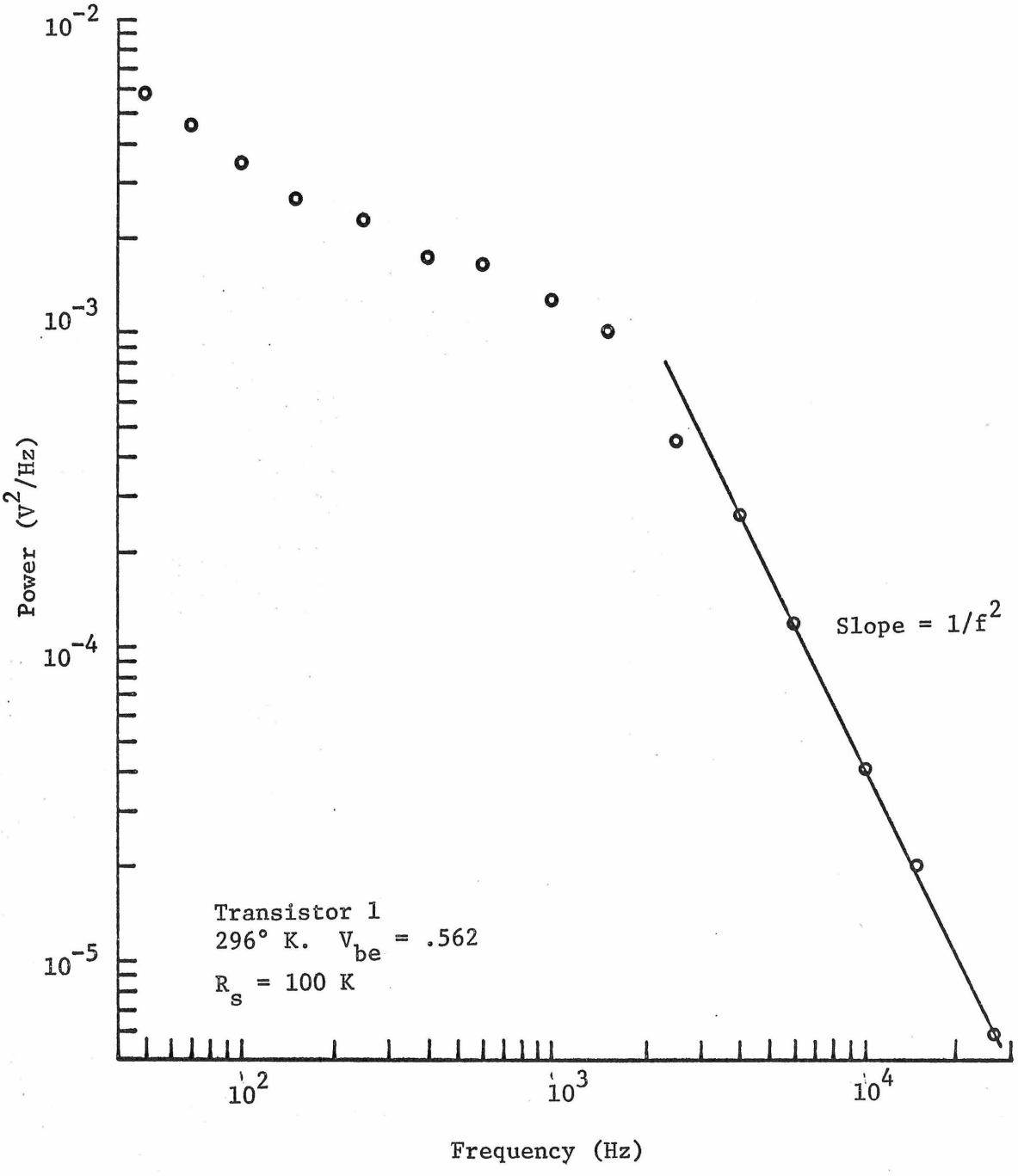

Figure 23. Burst Noise Power Spectral Density

test was made with an integrated circuit whose low frequency spectrum with a certain source resistance was known to be essentially flat. That knowledge was based on a digital spectral estimate and on spot noise readings at 10, 100 and 1000 Hz using a Quan-Tech model 2181 transistor noise test unit. The wave analyzer indicated the 50 Hz noise was nearly three times greater than that at 250 Hz, and the intermediate values diminished accordingly, using an experimental configuration corresponding to that of Figure 23. The second confirmation of the spuriousness of the low frequency values in the graph is based on an independent digital spectral estimate. An examination of the spectrum in the region below 500 Hz yielded the results indicated in Figure 24, which also has points above 500 Hz from the previous figure. The spectrum is quite flat in the decade 50-500 Hz, in conflict with the questionable prior measurement. Furthermore, the slow rise in amplitude from 500 to 1 Hz is subtle and may not be a characteristic of the burst noise.

The results to this point appear to indicate two items: the form of the burst noise spectrum, and the fact that published information has been incomplete and occasionally misleading. Undoubtedly the high frequency dependence of the spectrum is as $1/f^2$. At the other extreme the spectrum seems flat, but further investigation is required. If such a frequency dependence proves supportable, perhaps the burst noise spectrum closely matches that of the random telegraph wave, regardless of whether τ_1 and τ_0 are equal.

To examine the burst noise power spectrum more carefully, another transistor was chosen which exhibited a well defined burst

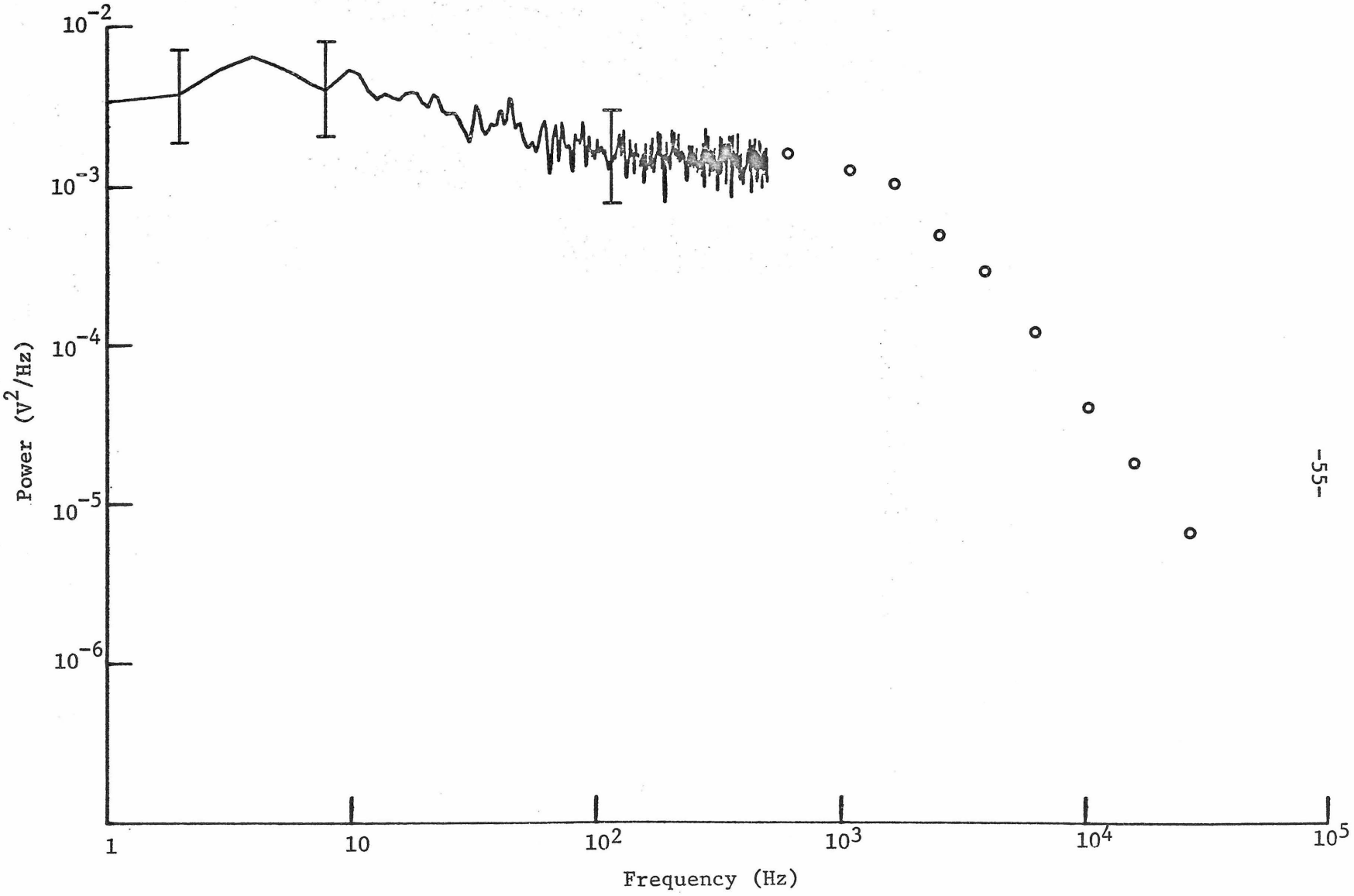
10^{-2}
10^{-3}
10^{-4}
10^{-5}
10^{-6}
Power (V^2/Hz)
1
10
10^2
10^3
10^4
10^5
Frequency (Hz)

Figure 24

mechanism and had somewhat longer durations. THe latter property seemed desirable in view of the upper frequency limit of the available apparatus. Furthermore, the noise was conditioned by using the previously described Schmitt trigger to square up the pulses in hopes of eliminating the effects of the remaining noise. It is possible that 1/f noise of a smaller burst noise source caused the slight linear trend at low frequencies in Figure 24.

The experiment entailed measurements with the wave analyzer at a number of frequencies within its range and two digital estimates, one 500 Hz and below and the other 5 Hz and below. In Figure 25 the results are presented with a theoretically predicted power spectrum whose whose origins and significance will be treated in the next chapter. The three varieties of measurement do not match up particularly well, but indicate the form of the power spectrum satisfactorily. Below 2 Hz the spectrum is flat; above 20 Hz the trend is $1/f^2$. In all likelihood the lower frequency digital estimate is uniformly high because of the effect of aliasing, which is the translation of unwanted frequencies down to the measurement frequency by the sampling process. Aliasing is responsible for the minor leveling off of the slope in the upper frequencies of the higher frequency digital estimate. The wave analyzer data points follow a slope consistent with other results, although prior difficulties with the system might lead one to suspect the values of being uniformly high. In spite of such difficulties, the magnitudes, break point, and frequency dependence are consistent and sufficiently well documented. One concludes that burst noise has a power spectrum

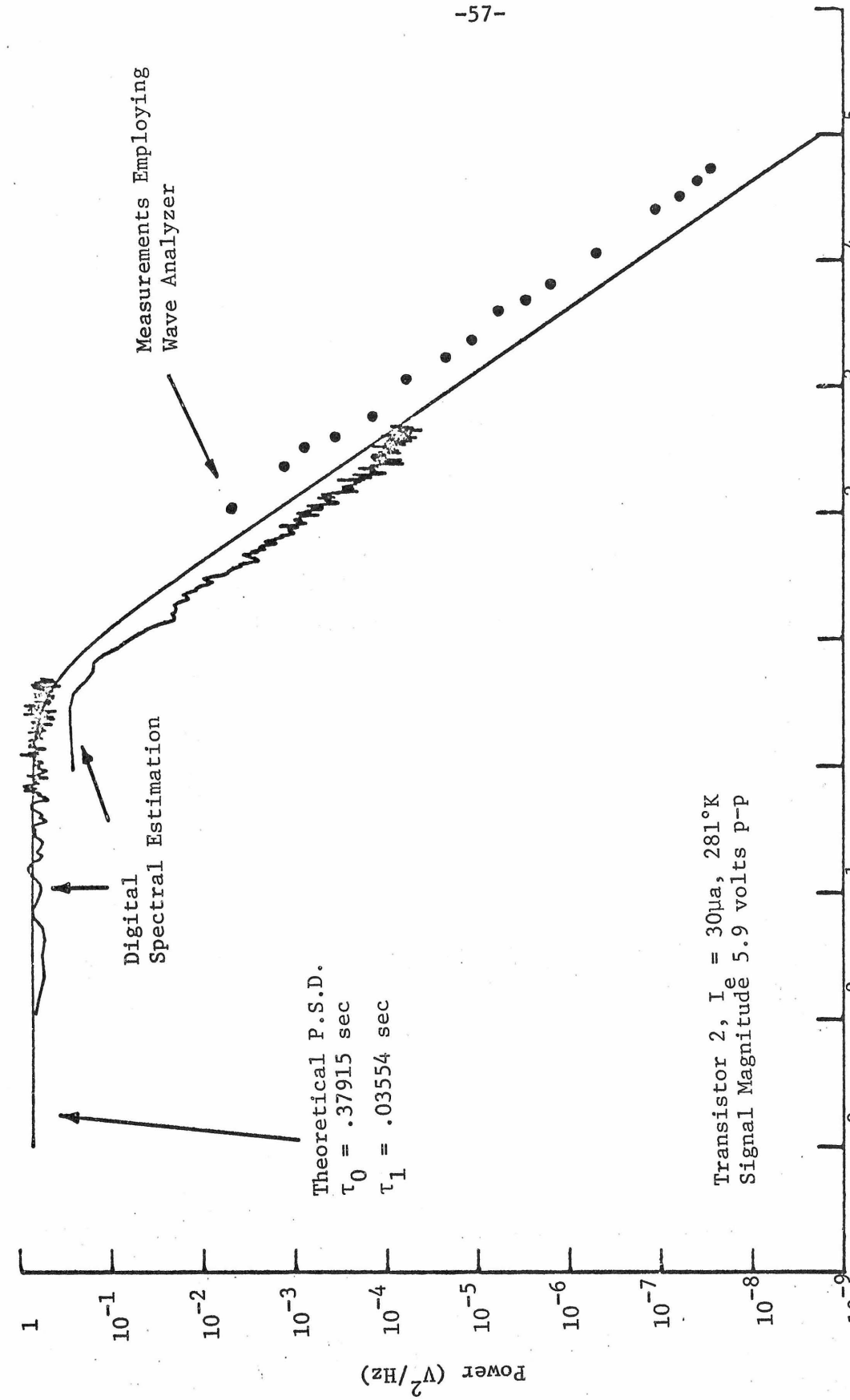

Figure 25. Burst Noise Power Spectral Density

which is flat at low frequencies and diminishes as $1/f^2$ at high frequencies.

CHAPTER VII

THEORETICAL BURST NOISE POWER SPECTRUM

We expect the burst noise power spectral density to be identical with that of a random telegraph wave if $\tau_1 = \tau_0$, but for the general case of inequality there is little information. The only attempt in the literature to solve this problem is due to Hsu (6), who followed a procedure outlined by Van der Ziel (16) for a sequence of identical pulses occurring randomly in time. In principle, one can obtain the Fourier transform for a single pulse and then apply "Carson's theorem" (term used by Van der Ziel) to arrive at the spectrum of a summation of pulses. Hsu's result has the form

$$S(\omega) = C\left[\frac{\sin \omega\tau}{\omega\tau}\right]^2$$

which is a periodic function whose envelope is flat at low frequencies and then tapers off as $1/f^2$. Presumably the Carson referred to is J.R. Carson (17), whose work on power spectra of noise is now classic. Carson made an assumption regarding the summation of pulses which required them to add linearly, that is, two pulses occurring at the same time are equivalent to one pulse of double height. In the case of burst noise, two pulses simply cannot be simultaneous. Moreover, the simplification that the pulses are identical transforms the problem entirely. Consequently, Hsu predicted a behavior of the correct low frequency form, but the ensuing periodicity at high frequencies, we feel intuitively, must be incorrect for any process random in time. To be sure, it cannot

apply to the known case of equal duration time constants.

To those familiar with the field of communication theory it should be, in principle, a comparatively straightforward matter to derive the power spectrum of any stationary random process whose statistics are adequately known. Sufficient knowledge exists regarding burst noise. As it occurred, the primary obstacles to obtaining the spectrum were choosing and precisely defining probabilities and finding functional forms for integrals and sums. In the discussion that follows, there will first be a brief statement concerning the notation, then the problem will be defined and solved.

We shall have occasion to speak of the probability of an event. The form to be used is $P\{y \geq \alpha\}$, where the event is set off by braces and in this case means the random variable y is greater than or equal to the number α. Probability densities will employ the lower case, _e.g._ $p_1(\tau)$. The expected value of a random variable x will be denoted by $E(x)$ and defined as

$$E(x) = \int_{-\infty}^{\infty} z\, p(z)\, dz$$

where $p(z)$ is the probability density function for x. $E(x)$ means the ensemble average of x over its permissible values. Therefore, if the values are discrete instead of continuous, $E(x)$ becomes

$$E(x) = \sum z_n\, P\{x = z_n\}$$

where z_n are the allowable values of x. The latter expression for

$E(x)$ uses the probabilities for each value of x. It is consistent to view $p(z)$, the probability density for x in the former expression, as a localized probability, or

$$P\left\{ z \leq x \leq z + dz \right\} = p(z)\, dz$$

In order to obtain a closed form expression for the power spectral density (PSD) of burst noise, the procedure must be based on the definition of PSD as the Fourier transform of the autocorrelation function of our process. Consequently we must obtain a useful formulation of the autocorrelation function from the known statistics of burst noise.

In the chapter on time domain characteristics, the expressions for the probability densities of the pulse durations were empirically derived:

$$p_1(t) = \frac{1}{\tau_1} e^{-\frac{t}{\tau_1}} \qquad p_0(t) = \frac{1}{\tau_0} e^{-\frac{t}{\tau_0}}$$

These expressions are consistent with the physical model, which entails a decay-like process. The random variable t is the length of time the noise remains in whichever state is being considered. On the basis of the densities, we must ultimately arrive at the PSD of burst noise, which is a generalized random telegraph wave, by deriving its autocorrelation function and taking the Fourier transform. Note that the random telegraph wave has a single expression describing the time between transitions, while burst noise has two: $p_1(t)$ and $p_0(t)$.

First, an important property of the burst noise process will be derived.

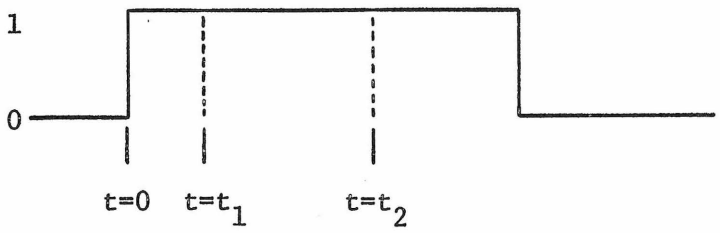

Assume the process $x(t)$ becomes 1 at time $t = 0$. The probability that $x(t)$ has not made a transition to 0 by a later time t_1 is

$$P\left\{\text{duration of } x \text{ is} > t_1\right\}$$

$$= \int_{t_1}^{\infty} p_1(t)\, dt = e^{-\frac{t_1}{\tau_1}} .$$

Given that $x(t)$ still is 1 at time t_1 and first became 1 at time $t = 0$, the probability that $x(t)$ hasn't changed by a later time t_2 is

$$P\left\{x(t_2) \text{ is still 1 given } x(t_1) \text{ was still 1}\right\}$$

$$= \frac{P\left\{\text{duration of } x \text{ is} > t_2\right\}}{P\left\{\text{duration of } x \text{ is} > t_1\right\}}$$

$$= e^{-\frac{t_2 - t_1}{\tau_1}}$$

which is a function only of the difference between t_1 and t_2. Therefore probabilities at time t_2 may be calculated from a knowledge of $x(t_1)$ irrespective of events prior to t_1. Since the probability of

a transition relies solely on the length of time considered, regardless of how recent the last transition was, apparently the probability of a transition is the same at each point in time. The property useful to us is that we need not begin probability computations at a transition.

We intend to obtain an expression for the autocorrelation function of x, $R_x(T)$, which can subsequently be used to produce the spectrum. Since x has only two values, there are four terms in the function.

$$\begin{aligned} R_x(T) &= 0\cdot 0\cdot P\left\{x(t) = 0,\ \ x(t+T) = 0\right\} \\ &\quad + 1\cdot 0\cdot P\left\{x(t) = 1,\ \ x(t+T) = 0\right\} \\ &\quad + 0\cdot 1\cdot P\left\{x(t) = 0,\ \ x(t+T) = 1\right\} \\ &\quad + 1\cdot 1\cdot P\left\{x(t) = 1,\ \ x(t+T) = 1\right\} \\ &= P\left\{x(t) = 1,\ \ x(t+T) = 1\right\} \end{aligned}$$

The expression is rendered more useful by the previously used substitution regarding conditioned probabilities:

$$R_x(T) = P\left\{x(t) = 1\right\}\ \ P\left\{x(t+T) = 1 \ \text{ given } x(t) = 1\right\}$$

The first term is straightforward. Since the expected pulse widths are τ_1 and τ_0, the probability that x equals 1 is clearly $\tau_1/(\tau_1 + \tau_0)$. The challenge is to evaluate the second term.

Because the problem is invariant under time axis translation, we shall write the quantity we seek as

$$P\left\{ x(T) = 1 \quad \text{given } x(0) = 1 \right\}$$

Consider a burst noise waveform in state 1 at time 0.

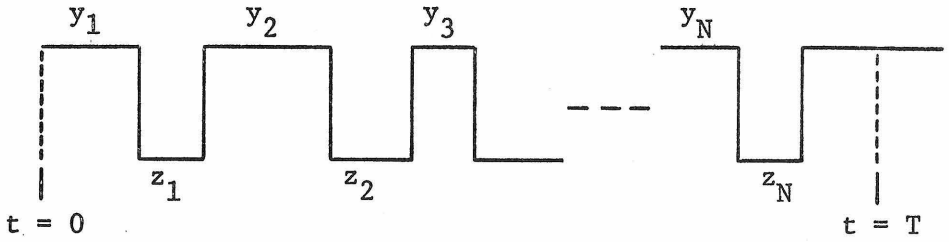

In order for the wave to be in state 1 at time T, there must be an even number of transitions in the interval (0,T). We shall assume there are 2N transitions where N may be any non-negative integer and denote the 1 state durations by y_i and those of 0 by z_i. The final pulse width in the 1 state must be at least the difference between T and the sum of the y_i and z_i to ensure that the state is 1 at time T, i.e. $x(t) = 1$ for $t = T$ and changes to 0 at some unspecified time later.

Under the following definitions

$$Y = \sum_{i=1}^{N} y_i \qquad Z = \sum_{i=1}^{N} z_i$$

we must find the probability density functions of Y and Z in order to describe the statistics of burst noise in a more useful form. For a given value of N, let the probability density of Y be denoted by $p_1^N(Y)$, where the subscript indicates the presence of the time constant τ_1. The case of $N = 1$ is already known:

$$p_1^1(Y) = p_1(Y) = \frac{1}{\tau_1} e^{-\frac{Y}{\tau_1}}$$

as the probability density of the single event has been found to be exponential. If $N = 2$, $Y = y_1 + y_2$, where the latter two random variables are independently selected from the same exponential population. It is known (see Papoulis (14), for example) that if y_1 and y_2 are independent, the probability density of their sum equals the convolution of their densities. Specifically,

$$p_1^2(Y) = p_1(Y) * p_1(Y) = \int_0^Y p_1(Y - t) \cdot p_1(t)\, dt$$

$$= \frac{1}{\tau_1^2} \int_0^Y e^{-(Y-t)/\tau_1} e^{-t/\tau_1}\, dt = \frac{Y}{\tau_1^2} e^{-Y/\tau_1} .$$

When $N = 3$, we may convolve with the previous result.

$$p_1^3(Y) = p_1(Y) * p_1^2(Y) = \frac{1}{\tau_1^3} \int_0^Y t\, e^{-(Y-t)/\tau_1} e^{-t/\tau_1}\, dt$$

$$= \frac{Y^2}{2\tau_1^3} e^{-Y/\tau_1}$$

To prove the general case by induction, we shall assume for any positive integer N the probability density is given by

$$p_1^N(Y) = \frac{Y^{N-1}}{\tau_1^N (N-1)!} e^{-Y/\tau_1} .$$

The proof for the case $N + 1$ entails only a straightforward integration:

$$p_1^{N+1}(Y) = p^N(Y) * p_1(Y) = \frac{1}{\tau_1^N (N-1)!} \int_0^Y t^{N-1} e^{-t/\tau_1} \frac{1}{\tau_1} e^{-(Y-t)/\tau_1} dt$$

$$= \frac{Y^N}{\tau_1^{N+1} N!} e^{-Y/\tau_1}$$

Note that this result is equivalent to the assumed expression for $p_1^N(Y)$ except that N is replaced by $N + 1$. Thus the formula for $p_1^N(Y)$ is proven by induction for integral, positive N. Obviously $p_0^N(Z)$ has an identical form, with the time constant of τ_0.

Recall that the problem at hand is to derive the probability

$$P\left\{ x(T) = 1 \quad \text{given} \quad x(0) = 1 \right\}$$

where $x(t)$ is the burst noise process as discussed four pages previously. The approach is the conceptually straightforward one of computing the probability of a burst noise waveform as illustrated on page 64 starting and ending in state 1 and having N positive and N negative transitions irrespective of the actual lengths of the y_i and z_i. We have the probability densities for the sum of N y_i and the sum of N z_i, i.e. for Y and Z. By convolution we shall determine the density of $Y + Z$. The integration of this density over the permissible values of $Y + Z$ plus an integration for the final duration in the 1 state gives the probability of the waveform. That is, denoting $Y + Z$ as s, we have the probability density $f^N(s)$

$$f^N(s) = p_1^N(s) * p_0^N(s)$$

which applies to the event of N double transitions in time s and beginning and ending in state 1. After the last transition the waveform remains in state 1 until at least time T, which is equivalent to stating that the final 1 state duration lies between the values of $T-s$ and ∞. This final duration is independent of previous events. Therefore the probability density for the complete waveform from $t = 0$ to $t = T$ is merely the product of $f^N(s)$ and the density of the last duration:

$$f^N(s)\, p_1(w) = f^N(s)\, \frac{e^{-w/\tau_1}}{\tau_1}$$

which is a joint density in s and w, where w is the random variable representing the final 1 state duration. Consequently, the probability of a burst noise waveform ending in state 1 at time T (given state 1 at time 0) and having N double transitions between those times is:

$$P^N(T) = \int_{s=0}^{T} \int_{w=T-s}^{\infty} f^N(s)\, \frac{e^{-w/\tau_1}}{\tau_1}\, dw\, ds\ .$$

Recall that s is the sum of the y_i and z_i and that it may range from 0 to T. The variable w is the time in the 1 state following the Nth positive transition and must be a minimum of T-s. In principle all that remains is to perform the indicated integrals and sum the resulting probabilities to obtain the result:

$$P\left\{x(T) = 1 \quad \text{given} \quad x(0) = 1\right\} =$$

$$= P\left\{x \text{ remaining 1 over } (0,T)\right\} + \sum_{N=1}^{\infty} P^N(T) .$$

The integrals are in fact tractable, and consequently a closed form solution was obtained. However, the form for $P^N(T)$ entailed a double finite sum of exponentials having such complicated coefficients that after a good deal of effort little hope was held for executing the infinite sum and reaching a usable answer.

Fortunately, an alternative route was discovered which required the infinite sum to be done at an earlier stage and allowed the finite sums to be avoided altogether. We had required the expression for the density

$$f^N(s) = p_1^N(s) * p_0^N(s) = \int_0^s p_1^N(t)\, p_0^N(s - t)\, dt$$

$$= \int_0^s \frac{t^{N-1}\,(s - t)^{N-1}\, e^{-t/\tau_1}\, e^{-(s - t)/\tau_0}}{\tau_1^N\, \tau_0^N\, (N-1)!^2}\, dt ,$$

but rather than performing the integration on t, we shall first sum the integrand on N. Presumably the exchange of integration and summation is legitimate as the function is well behaved and the results will be found to converge. That part of the integrand dependent on N, when summed is

$$\sum_{N=1}^{\infty} \frac{[t(s-t)]^N}{(\tau_1\tau_0)^N (N-1)!^2} \quad .$$

The factorial squared coefficient was not immediately located in the standard tables of infinite series. However, two differentiations and a modicum of algebra yielded a simple differential equation from which the form of the sum was ascertained. As it occurred, the solution was a Bessel function of complex argument. Let $f(s)$ represent the sum of the $f^N(s)$.

$$f(s) = \sum_{N=1}^{\infty} f^N(s) = \frac{e^{-s/\tau_0}}{\tau_1\tau_0} \int_0^s \left[\sum_{N=1}^{\infty} \left\{ \frac{t(s-t)}{\tau_1\tau_0} \right\}^{N-1} \frac{1}{(N-1)!^2} \right] e^{-t(1/\tau_1 - \frac{1}{\tau_0})} dt$$

$$= \frac{e^{-s/\tau_0}}{\tau_1\tau_0} \int_0^s I_0\left(2\sqrt{\frac{t(s-t)}{\tau_1\tau_0}} \right) e^{-t(1/\tau_1 - \frac{1}{\tau_0})} dt \quad .$$

On first appearances, this form appears no more useful than might a double finite sum. There are no entries in the standard extensive integral tables having a sufficient resemblance. Fortuitously however, a Laplace transform pair involving the Bessel function J_o in a related integral was located in the classic work of Magnus and Oberhettinger

(18). By suitable substitutions the tabulated expression was brought into agreement with our integral, and then the transform of the expression was inverted with the result that

$$\int_0^t I_0 \left[a\sqrt{x(t-x)}\right] e^{-bx}\, dx = \frac{2e^{-\frac{bt}{2}}}{\sqrt{b^2+a^2}} \sinh \frac{\sqrt{b^2+a^2}}{2}\, t \ .$$

This simple result apparently is not obtainable by any but a circuitous route; the result's validity is demonstrated in Appendix II by a transform technique which renders the proof interesting in its own right.

Having solved the integral, the solution for $f(s)$ is

$$f(s) = \frac{2e^{-\frac{s}{2}\left(\frac{1}{\tau_1}+\frac{1}{\tau_0}\right)}}{\tau_1+\tau_0} \sinh \frac{s}{2}\left(\frac{1}{\tau_1}+\frac{1}{\tau_0}\right) \ .$$

Therefore

$$\sum_{N=1}^{\infty} P^N(T) = \int_{s=0}^{T} \int_{w=T-s}^{\infty} f(s)\, \frac{e^{-w/\tau_1}}{\tau_1}\, dw\, ds = e^{-T/\tau_1} \int_{s=0}^{T} f(s)\, e^{s/\tau_1}\, ds$$

$$= \frac{2e^{-T/\tau_1}}{\tau_1+\tau_0} \int_{s=0}^{T} e^{-\frac{s}{2}\left(\frac{1}{\tau_0}-\frac{1}{\tau_1}\right)} \sinh \frac{s}{2}\left(\frac{1}{\tau_1}+\frac{1}{\tau_0}\right) ds$$

$$= \frac{\tau_1+\tau_0}{\tau_1+\tau_0}\, e^{-T\left(\frac{1}{\tau_1}+\frac{1}{\tau_0}\right)} - e^{-T/\tau_1} \ .$$

This formula is not yet directly applicable to the burst noise waveform

as we have neglected to consider the probability of no transition in the interval (0,T). The missing term is straightforward to compute:

$$P\left\{\text{no transition from state 1 in interval } (0,T)\right\}$$

$$= P\left\{\text{first transition is in interval } (T,\infty)\right\}$$

$$= \int_T^\infty \frac{1}{\tau_1} e^{-t/\tau_1}\, dt = e^{-T/\tau_1} \quad .$$

Adding that term to the probabilities previously summed gives the probability that the burst noise waveform beginning in state 1 also ends in state 1:

$$P(T) = \frac{\tau_1 + \tau_0\, e^{-T\left(\frac{1}{\tau_1} + \frac{1}{\tau_0}\right)}}{\tau_1 + \tau_0} \quad .$$

To obtain the autocorrelation function it is only necessary to multiply P(T) by the probability that the waveform began in the 1 state.

$$R_x(T) = \frac{\tau_1}{\tau_0+\tau_1} P(T) = \frac{\tau_1^2 + \tau_1\tau_0\, e^{-T\left(\frac{1}{\tau_1} + \frac{1}{\tau_0}\right)}}{(\tau_1 + \tau_0)^2}$$

The final point to be considered prior to arriving at the power spectrum is a brief one that has not been previously mentioned. The waveform proposed has the permissible levels of 0 and 1; these may be interpreted as voltage levels, say 0 and 1 volt, since we are in fact considering an electrical signal. Note then that the signal

has a d.c. component of $\tau_1/(\tau_1+\tau_0)$ volts. The d.c. introduces an impulse function into the power spectrum at zero frequency. To avoid this complication, we shall subtract that portion of $R_x(T)$ corresponding to the d.c. component of the waveform. The autocorrelation function of a constant is simply the constant squared. Therefore the autocorrelation function for the a.c. burst noise waveform is

$$\frac{\tau_1\tau_0\, e^{-T\left(\frac{1}{\tau_1}+\frac{1}{\tau_0}\right)}}{(\tau_1+\tau_0)^2} \quad .$$

Subtraction of the constant term may appear inelegant, but we seek the spectrum of an a.c. signal, and the presence of d.c. is a trivial matter. An alternative procedure would be to begin with a wave having no constant component, but the ensuing algebra would be significantly more cumbersome than that we have encountered.

We now arrive at the power spectrum of burst noise:

$$S(\omega) = \frac{\tau_1\tau_0}{(\tau_1+\tau_0)^2} F\left[e^{-T\left(\frac{1}{\tau_1}+\frac{1}{\tau_0}\right)}\right]$$

$$= \frac{2\tau_1\tau_0}{(\tau_1+\tau_0)^2} \int_0^\infty \cos \omega T \; e^{-T\left(\frac{1}{\tau_1}+\frac{1}{\tau_0}\right)} \, dT$$

$$= \frac{2}{(\tau_1+\tau_0)\left[\left(\frac{1}{\tau_1}+\frac{1}{\tau_0}\right)^2+\omega^2\right]} \quad .$$

We recognize immediately that this elegantly simple result has the form of a random telegraph wave: flat at low frequencies, subsequently decreasing as $1/f^2$. The expression is symmetrical in τ_1 and τ_0 as one expects (for example, interchanging the 1 and 0 levels will not disturb the PSD). Furthermore, when $\tau_1 = \tau_0$, the spectrum is exactly that of the random telegraph wave.

Figure 26 illustrates the functional properties of our epxression for the burst noise PSD. The constant τ_0 is set to 1 sec while τ_1 is treated as a parameter. The greatest low frequency power density appears on the $\tau_1 = 2$ sec plot, although its high frequency power falls below that of $\tau_1 = 1$ sec, and consequently its total power is less than that for $\tau_1 = 1$ sec. Maximum total power occurs for the condition $\tau_1 = \tau_0$ as one might expect. Total power versus the ratio of τ_1 to τ_0 is plotted in Figure 27, clearly indicating a maximum at the predicted point.

A return glance at Figure 25 supports the accuracy of the theoretical burst noise PSD. That expression is plotted with the experimental results by obtaining values for the amplitude, τ_1 and τ_0 from the tape recorded data. The excellent agreement of theory with reality constitutes sound evidence for the validity of our derivation.

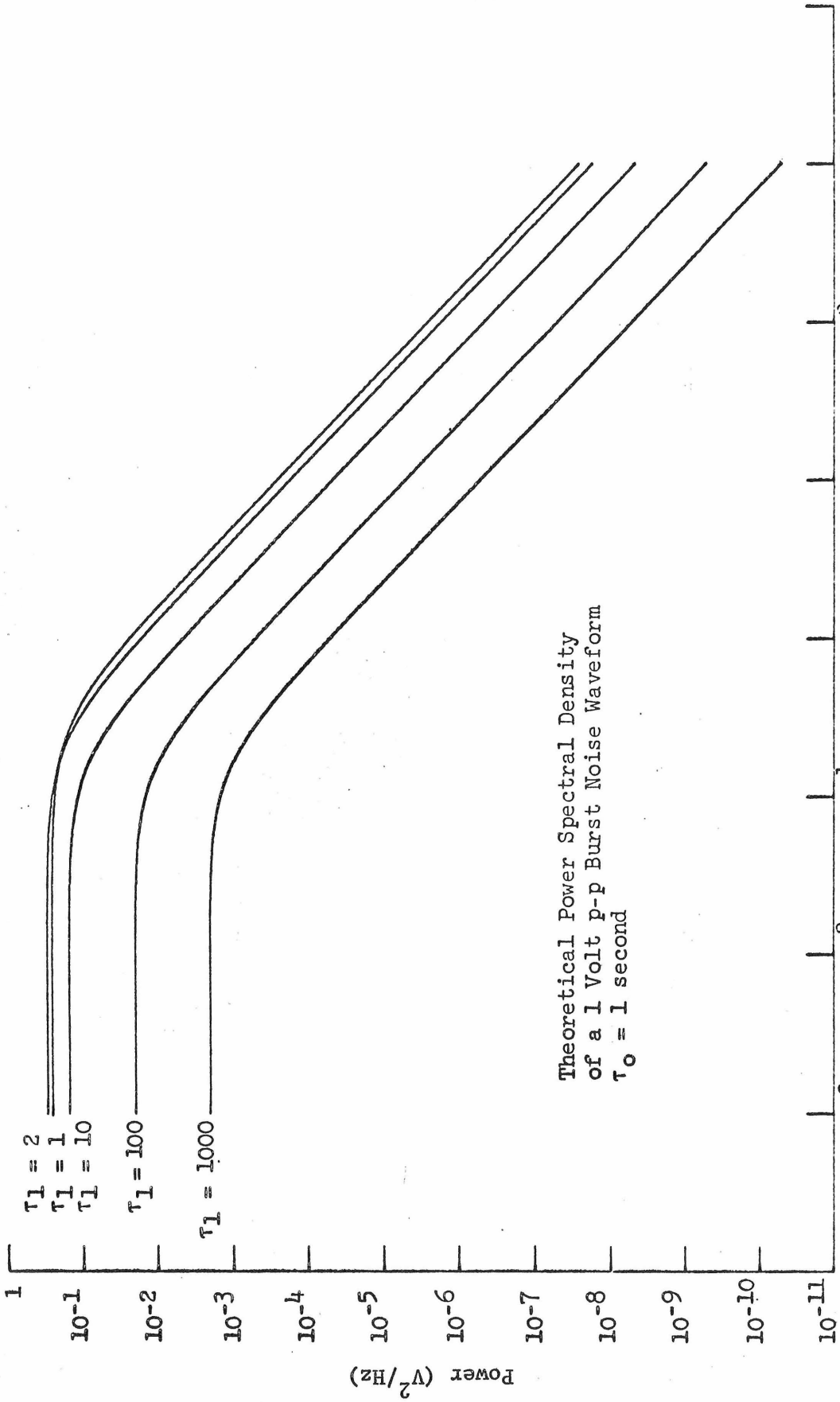
Power (V^2/Hz)
1
10^{-1}
10^{-2}
10^{-3}
10^{-4}
10^{-5}
10^{-6}
10^{-7}
10^{-8}
10^{-9}
10^{-10}
10^{-11}
$\tau_1 = 2$
$\tau_1 = 1$
$\tau_1 = 10$
$\tau_1 = 100$
$\tau_1 = 1000$
Theoretical Power Spectral Density
of a 1 Volt p-p Burst Noise Waveform
τ_o = 1 second
10^{-3} Hz
10^{-2}
10^{-1}
1
10
10^2
10^3
Frequency (Hz)

Figure 26.

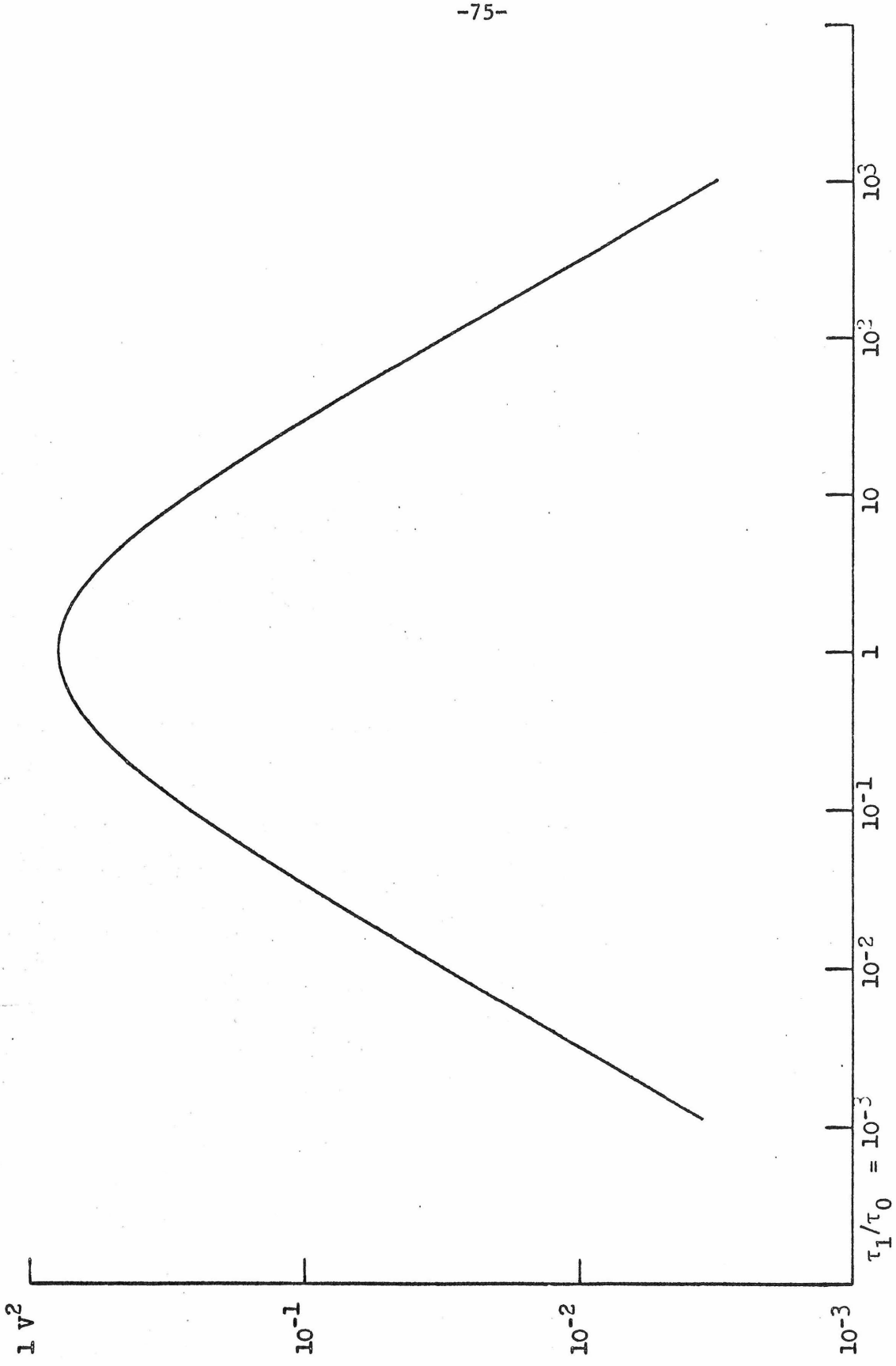

Figure 27. Theoretical Power of a 1 Volt p-p Burst Noise Waveform

CHAPTER VIII

SUMMARY OF FINDINGS

This section is intended to list those facts which are theoretically derived or experimentally uncovered in this research on burst noise in bipolar transistors and linear integrated circuits. The noise exhibits itself as one or more rectangular waveforms, each having a constant peak to peak amplitude but random pulse duration.

Burst noise is not Gaussian. Measurements on the percentage of time the noise spends at each of its permissible values indicate a bimodal amplitude distribution. Estimation of the amplitude distribution was found to be a powerful tool in establishing the presence of burst noise in a given source.

The amplitude of burst noise has been found to vary with the parameters: base-emitter voltage, temperature, and source resistance. It is invariant under collector-emitter voltage change. The linear dependence of noise amplitude on source resistance over a wide range of the latter implies an equivalent circuit of a current source shunted across the base-emitter junction. Observed magnitudes of the noise range from 10^{-10} to nearly 10^{-6} ampere p-p.

Pulse durations of the noise have been found as short as 10 μsec and as long as some 29 hours, with typical average values of 1 msec. Careful measurements on the relative frequency with which the pulse occurred in a sample gave a duration probability density of $\frac{1}{\tau} e^{-\frac{t}{\tau}}$, where t is duration.

One concludes that burst noise originates in the base-emitter junction because the various electrical parameters regarding that junction influence the noise. The constancy of noise amplitude eliminates the possibility of number of particles acting in unison being the cause of burst noise. Furthermore, the duration statistics are those of a single particle alternately being trapped and escaping. The proposal that the noise originates in trapping is due to Mead and Whittier; only evidence in support of that theory has been found in this work. The manner in which the mean pulse durations vary with base-emitter voltage is consistent with trapping. Furthermore, duration versus temperature measurements indicate activation energies of about .4 to .5 volts, values corresponding to a trap roughly in the middle of the silicon band gap.

Suggestions in the literature for the form of the burst noise power spectrum have been inconsistent. However, careful measurements by this experimenter have demonstrated that the spectrum is flat at low frequencies but falls as $1/f^2$ at higher ones. The dependence is precisely that of the classic random telegraph wave. That well known wave has a spectrum which is simple to compute theoretically, but the next step of predicting the burst noise spectrum has heretofore not been taken. Nevertheless, the problem was solved here by deriving the autocorrelation function and taking the Fourier transform. The result matched experiment and the specific theoretical case of the random telegraph wave.

APPENDIX I

CIRCUITS DESIGNED FOR BURST NOISE EXPERIMENTS

Amplifier Configuration for Observation of Burst Noise in Grounded Emitter Transistor

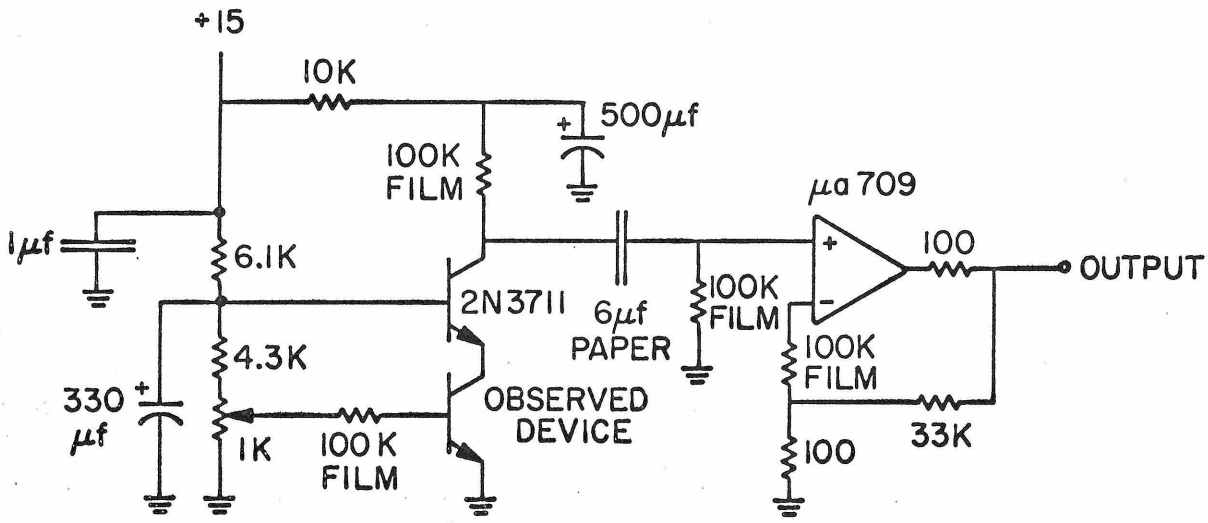

The high impedances and low currents desirable for these measurements are detriments to bandwidth. Therefore the cascode connection illustrated above was utilized to eliminate Miller capacitance, giving the overall circuit a risetime of less than 30 μsec.

Schmitt Trigger

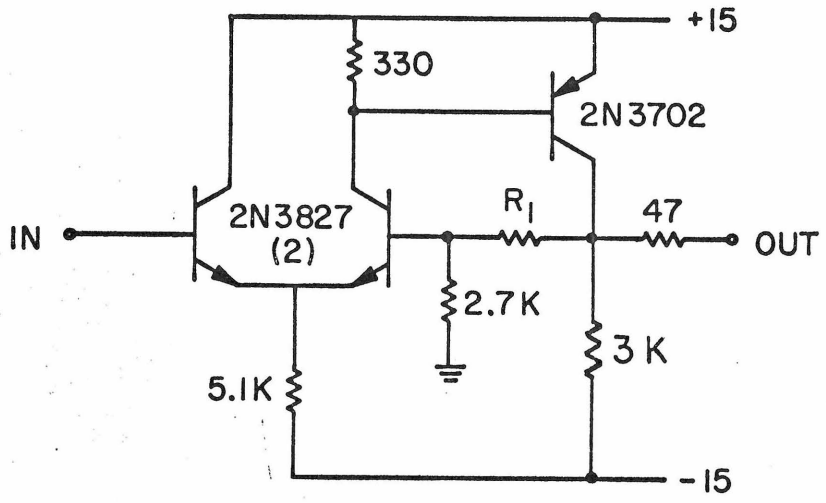

The amplifier output may be connected to the level detecting circuit above for the purpose of creating a clean rectangular waveform which is a replica of the original burst noise. The trigger levels are nearly symmetric about zero and are adjustable in that the hysteresis is directly dependent on R_1. For several experiments, the deadband was set at 1.6 volts (± .0.8) by choosing R_1 = 47k.

Typical Amplifier Configuration for Observation of Burst Noise in Integrated Circuits

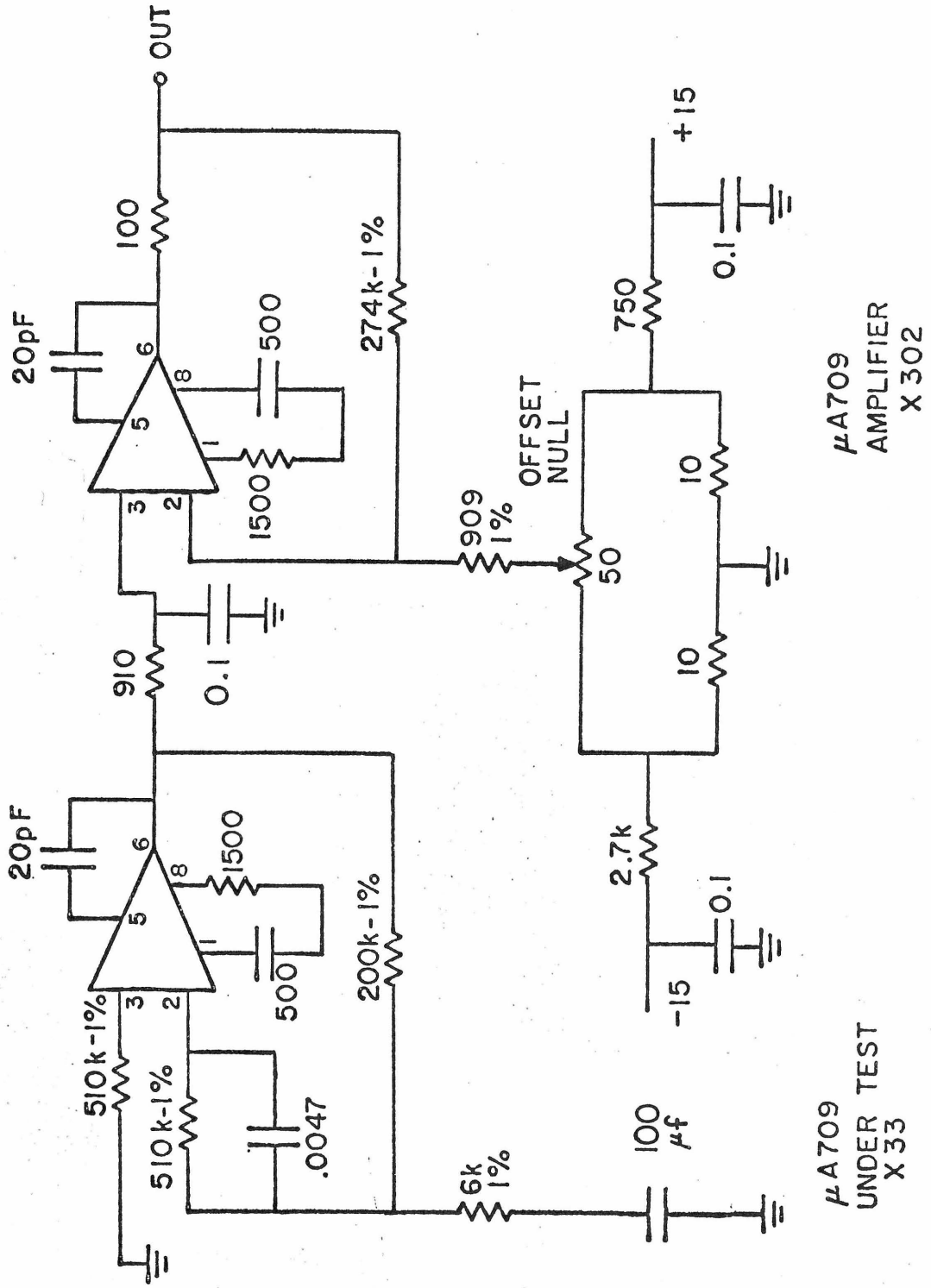

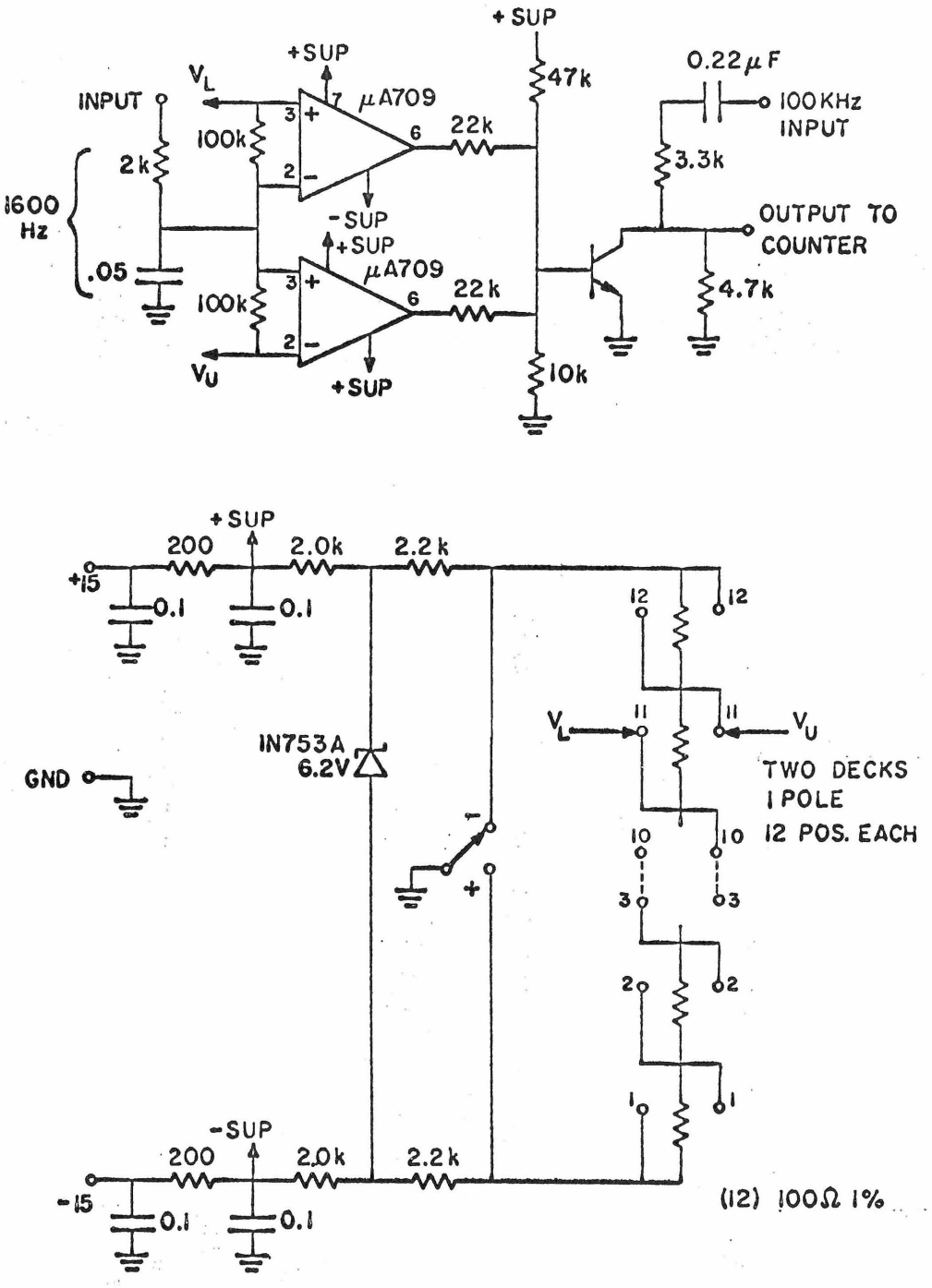

Noise Amplitude Distribution Circuit

The noise amplitude distribution circuit, in conjunction with an electronic counter, makes possible measurements regarding the distribution of amplitudes in a signal. The plots in Chapter III demonstrating that burst noise is multimodal rather than Gaussian were made using this equipment.

In brief, the circuit consists of two sections: a voltage reference and a comparison gate. The former supplies two potentials one ranging from -1.2 to +1.1 volt and the other always a 0.1 volt higher. The summed output of the comparator amplifiers is positive unless the input signal is between the two reference potentials. When the latter condition is satisfied, the summed output is negative and the gate transistor is cut off, enabling the 100 kHz reference signal to reach the counter. Otherwise, the transistor has forward base bias and presents a low impedance path to ground for the 100 kHz signal. Note that collector bias is neither present nor necessary. Operating the counter for a fixed period, e.g. 10 seconds, permits an accurate measurement of the fraction of time the noise spends at voltage levels between the selected two reference potentials.

Gated Oscillator Circuit for Average Pulse Duration Measurements

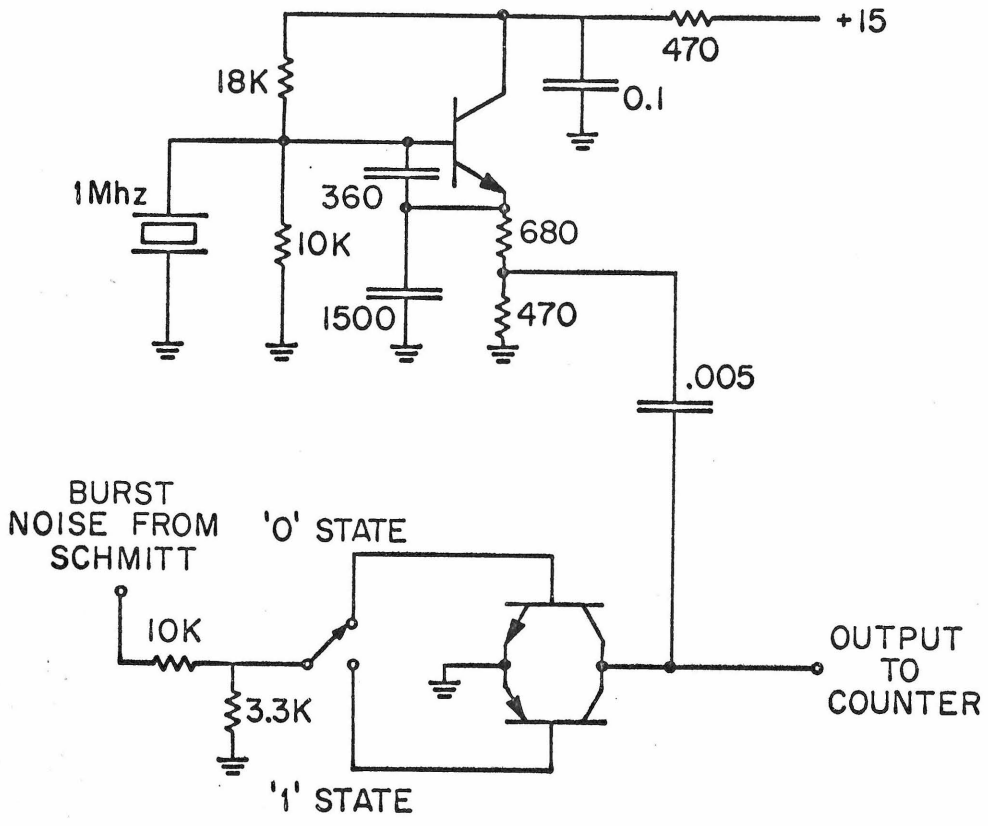

With the switch in the position shown, the 1 MHz signal is allowed to reach the counter only when the noise input is negative. Therefore, counting for a fixed period of time yields the average duty cycle quite accurately. This information is combined with the average frequency (measured directly with the counter) to produce the average duration. The switch is provided to determine positive and negative duty cycles separately, an aid in ensuring accuracy.

APPENDIX II

MATHEMATICAL DERIVATIONS

Evaluation of the Integral

$$I(t) = \int_0^t I_0 \left[2\alpha \sqrt{x(t-x)}\right] e^{-\beta x} \, dx$$

The closed form result was first derived by suitable substitution in a related form due to Magnus and Oberhettinger. That tabulated expression appeared as an entry in their Laplace transform table, for which a proof was suggested by Prof. J. N. Franklin. The evaluation that follows is a variation on the proof.

The Laplace transform:

$$L[I(t)] = \int_{t=0}^{\infty} e^{-st} \int_0^t I_0\left[(2\alpha \sqrt{x(t-x)}\right] e^{-\beta x} \, dx \, dt$$

Note $0 < x < t < \infty$, and interchange order of integration

$$= \int_{x=0}^{\infty} e^{-\beta x} \int_{t=x}^{\infty} e^{-st} \, I_0\left[(2\alpha \sqrt{x(t-x)}\right] dt \, dx$$

Let $t - x = \tau$

$$L[I(t)] = \int_{x=0}^{\infty} e^{-\beta x} \; e^{-sx} \int_{\tau}^{\infty} e^{-s\tau} \, I_0(2\alpha\sqrt{x\tau}) \; d\tau \, dx$$

Notice that the inner integral is itself a Laplace transform which may be found in tables or evaluated utilizing the series form for $I_0(z)$:

$$= \int_{x=0}^{\infty} e^{-x(\beta+s)} \sum_{k=0}^{\infty} \int_{\tau=0}^{\infty} e^{-s\tau} \frac{(\alpha^2 x\tau)^k}{(k!)^2} \, d\tau \, dx$$

$$= \int_{x=0}^{\infty} e^{-x(\beta+s)} \sum_{k=0}^{\infty} \frac{(\alpha^2 x)^k}{k! \, s^{k+1}} \, dx$$

$$= \int_{0}^{\infty} e^{-x(\beta+s)} \frac{1}{s} e^{\frac{\alpha^2 x}{s}} \, dx$$

$$= \frac{1}{s} \int_{0}^{\infty} e^{-x(\beta+s-\frac{\alpha^2}{s})} \, dx = \frac{1}{s^2 + \beta s - \alpha^2} .$$

The inverse transform may be found in tables or through a straightforward contour integration, as follows.

$$I(t) = \frac{1}{2\pi j} \int_{c-j\infty}^{c+j\infty} \frac{e^{st} \, ds}{s^2 + \beta s - \alpha^2}$$

There are two poles in the integrand:

$$S_+ = \frac{-\beta + \sqrt{\beta^2 + 4\alpha^2}}{2} , \qquad S_- = \frac{-\beta - \sqrt{\beta^2 + 4\alpha^2}}{2} .$$

Let us employ the contour $\Gamma_1\Gamma_2$ with the restriction $c > \text{Re}\,[S_+]$.

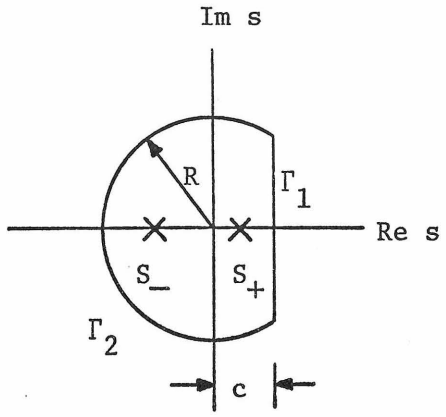

Since $t > 0$ and real, the integrand on Γ_2 is bounded,

$$\frac{|e^{st}|}{|(s-S_+)(s-S_-)|} \leq \frac{\exp[\max(\text{Re}(s))\cdot t]}{|(s-S_+)(s-S_-)|} \leq \frac{e^{ct}}{R^2}$$

and tends to zero as R approaches ∞.

Therefore, $I(t) = \sum \text{residues} = \dfrac{e^{S_+t}}{S_+-S_-} + \dfrac{e^{S_-t}}{S_--S_+}$

$$= \frac{e^{-\frac{\beta t}{2} + \frac{\sqrt{\beta^2+4\alpha^2}}{2}t}}{\sqrt{\beta^2+4\alpha^2}} - \frac{e^{-\frac{\beta t}{2} - \frac{\sqrt{\beta^2+4\alpha^2}}{2}t}}{\sqrt{\beta^2+4\alpha^2}}$$

$$= \frac{2e^{-\frac{\beta t}{2}}}{\sqrt{\beta^2+4\alpha^2}} \sinh \frac{\sqrt{\beta^2+4\alpha^2}}{2} t$$

which is the solution to the original integral.

The Standard Deviation in the Measurement of the Probability Density of Burst Noise Pulse Width

In Chapter IV two histograms are given, representing the number of pulses observed in each 25 μsec long range of duration. Overall, the plots are estimates of probability density function, but here we are concerned only with the number of measurements falling in a given range and the statistics of that number. The real probability density function is $p(t)$, shown as the smooth curve, and our estimate in the region t to $t + \Delta t$ is the rectangular histogram segment.

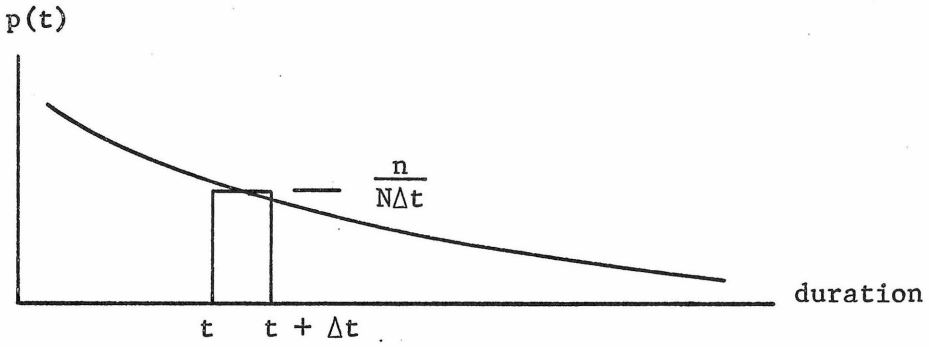

If N is the total number of measurements and n is the number of durations found to lie between t and $t + \Delta t$, then our estimate for the particular interval is $n/N\Delta t$. Now the actual probability of observing a duration within the region of interest in one attempt is

$$P = \int_{t}^{t+\Delta t} P(\tau)\, d\tau \quad .$$

The probability of a failure is $Q = 1 - P$. The probability of observing exactly one duration in the desired interval is

$$NPQ^{N-1} \quad ,$$

and the probability for two is

$$N(N-1)\ P^2 Q^{N-2}\ ,$$

et cetera.

This is the binomial distribution as one might expect of an experiment that consists of a sequence of identical trials, and furthermore,

$$P\left\{ n \text{ successes in } N \text{ trials} \right\} = \binom{N}{n} P^n Q^{N-n}\ .$$

The discrete random variable n is the quantity of interest, for which we shall obtain its mean μ and variance σ^2.

$$\mu = E(n) = \sum_{n=0}^{N} n\ p(n) = \sum_{n=0}^{N} n \binom{N}{n} P^n\ Q^{N-n}$$

$$= \sum_{n=1}^{N} \frac{N!}{(n-1)![N-1-(n-1)]!}\ P^n\ Q^{N-n}$$

$$= PN \sum_{n=1}^{N} \frac{(N-1)!}{(n-1)![N-1-(n-1)]!}\ P^{n-1}\ Q^{N-1-(n-1)}$$

substituting $z = n - 1$

$$= PN \sum_{z=0}^{N-1} \binom{N-1}{z} P^z\ Q^{N-1-z}$$

$$= PN$$

The preceding equality is seen to hold when we recognize that the final summation is merely $E(1)$ for the binomial distribution of $N-1$ trials.

The variance is

$$\sigma^2 = E\left\{(n-\mu)^2\right\} = E\left\{n^2\right\} - E\left\{2n\mu\right\} + n^2$$

$$= E\left\{n^2\right\} - \mu^2$$

The value of $E\left\{n^2\right\}$ is found by a circuitous approach.

$$E\left\{n(n-1)\right\} = \sum_{n=0}^{N} n(n-1)\binom{N}{n} P^n Q^{N-n}$$

$$= P^2N(N-1) \sum_{n=2}^{N} \frac{(N-2)!}{(n-2)![N-2-(n-2)]!} P^{n-2} Q^{N-2-(n-2)}$$

let $z = n-2$

$$= P^2N(N-1) \sum_{z=0}^{N-2} \binom{N-2}{z} P^z Q^{N-2-z}$$

$$= P^2N(N-1)$$

Therefore $E\left\{n^2\right\} = P^2N(N-1) + E(n) = P^2N^2 - P^2N + PN = N^2P^2 + NPQ$

$$\sigma^2 = E\left\{n^2\right\} - \mu^2 = NPQ.$$

To assign a standard deviation to our experiment, we must use estimates of P and Q, since those quantities are not known. The most likely value of P, based on our results is surely the number of

successes divided by the number of trials.

$$\text{Estimate of } P = \frac{n}{N} \cdot$$

Therefore,

$$\sigma = \sqrt{NPQ} = \sqrt{n - \frac{n^2}{N}} \cdot$$

Recall that the original plot was normalized to integrate to unity, and consequently the standard deviation actually employed is

$$\sigma = \frac{1}{N\Delta t} \sqrt{n - \frac{n^2}{N}} \cdot$$

APPENDIX III

ESTIMATION OF POWER SPECTRAL DENSITY

Introduction

There is no question that power spectrum measurement is a useful analytic tool in numerous disciplines. The common technique of filtering an electrical signal and measuring the resultant voltage is invaluable, but limited to situations having adequately long, continuous records and having frequencies for which suitable filter networks may be synthesized.

In the case at hand we are interested in a band of frequencies low enough to bring about serious difficulties in creating the necessary group of filters. Consequently we use the method of estimating the frequency content of relatively short records as described by Blackman and Tukey in The Measurement of Power Spectra. Complete details are to be found therein; this appendix is merely a brief summary of the techniques we found useful.

Background Theory

The power spectrum of a stationary stochastic process is defined simply as the Fourier transform of its autocorrelation function.

$$P(f) = \int_{\infty}^{\infty} C(\tau)\, e^{-j2\pi f\tau}\, d\tau$$

The traditional form of the autocorrelation function is in terms of an

ensemble average

$$C(\tau) = E\left\{ [X(t) - \overline{X}] \cdot [X(t + \tau) - \overline{X}] \right\}$$

where $\overline{X} = E\{X(t)\}$. Unfortunately, this form of $C(\tau)$ is hardly useful since we never actually have access to an entire ensemble. Therefore one must assume the process is ergodic and the autocorrelation function is

$$C(\tau) = \lim_{T \to \infty} \frac{1}{T} \int_{-\frac{T}{2}}^{\frac{T}{2}} X(t) \cdot X(t + \tau)\, dt$$

Since $C(\tau)$ is an even function, the Fourier transform becomes a cosine transform:

$$P(f) = \int_{\infty}^{\infty} C(\tau) \cos 2\pi f\tau d\tau$$

In actual practice of course, the autocorrelation function can only be approximated, because only finite measurement periods are physically admissible. Thus we are restricted merely to estimating the autocorrelation function and thence the spectrum.

Techniques Used in Present Study

It is perfectly feasible to estimate the correlation in a continuous manner, albeit somewhat inconvenient. However, it is preferable to utilize a sampling technique, thereby reducing problems both of data storage and processing. Sampling, analog-to-digital conversion,

and digital recording are straightforward and leave the data in a form readily reducible by computer.

A few precautions must be observed because the nature of the sampling process leads to frequency folding (aliasing). The frequencies of the undesired components reside at $nf_s \pm f_o$ where n is an integer ≥ 1, f_s is the sampling rate, and f_o is the frequency being measured.

It is advantageous to quantize time by periodic sampling, because the integrals become summations, which may be accomplished quite naturally on a digital computer. The correlation of our process now changes to

$$C(R) = \frac{1}{N-R} \sum_{q=0}^{N-R} X(q) \cdot X(q+R)$$

$C(R)$ corresponds to the covariance at lag $R\Delta t$ where Δt is the sampling interval. The N points $X(q)$ are the sampled data points, the index q indicating time $q\Delta t$. The $C(R)$ are called mean lagged products and form our estimate of the covariance function.

To estimate the spectrum, it is merely necessary to transform the lagged products. The transformation employed (corresponding to Fourier) is of the finite cosine type. The so-called raw spectral estimate for frequency $\frac{R}{2M\Delta t}$ is

$$V(R) = 2\Delta t \left[C(o) + 2 \sum_{q=1}^{M-1} C(q) \cos \frac{qR\pi}{M} + C(M) \cos R\pi \right]$$

Note that the allowable values of R are restricted by M, $0 \leq R \leq M$, since the highest frequency we can estimate is one-half the sampling rate. At this point it is well to indicate a limitation on M. Obviously M may range to N before the lagged product formula fails, but it must be remembered that our data are a truncated reproduction of the actual process, and allowing R to range larger than a small part of N will accentuate the problem by effectively truncating the data for large lags. Therefore M is usually taken as 5 to 10% of N.

Returning to an earlier step for the moment, recall that the lagged products are only an approximation to the actual autocorrelation function of the process under study. It is possible to improve accuracy, at least from the viewpoint of power spectrum estimation, by multiplying the autocorrelation estimate by one of several possible even functions of τ, called lag windows. The difficult philosophy of selecting a suitable window is discussed adequately by Blackman and Tukey. We use a function suited to our purpose which was originated by Hann:

$$h(\tau) = \frac{1}{2} \left(1 + \cos \frac{\pi\tau}{M\Delta t}\right) \qquad \tau < M\Delta t$$

$$= 0 \qquad \tau \geq 0$$

The important characteristic of Hann's lag window is its effect on the power spectrum estimate, where it acts as a spectral window of roughly triangular shape. The spectral estimate

$$P(f) = \int_{\infty}^{\infty} C(\tau) \cdot h(\tau)\, e^{-j2\pi f\tau}\, d\tau$$

is equivalent, by the convolution theorem, to

$$P(f) = \int_{\infty}^{\infty} C(\pi)\, e^{-j2\pi f\tau}\, d\tau \;*\; \int_{\infty}^{\infty} h(\tau)\, e^{-j2\pi f\tau}\, d\tau$$

$V(R)$ is the transform in discrete time of $C(\tau)$; $H(R)$ may be used for the Fourier transform of $H(\tau)$ since only discrete points of time are used in the convolution. $H(R)$ yields a conveniently simple procedure for obtaining the final spectral estimates $U(R)$:

$$U(R) = H(R) * V(R) = \tfrac{1}{4}\, V(R-1) + \tfrac{1}{2}\, V(R) + \tfrac{1}{4}\, V(R+1)$$

Note the obvious spectrum smoothing property of $h(\tau)$. Naturally the above expression must be modified slightly when R assumes its minimum and maximum values.

$$U(0) = \tfrac{1}{2}\, V(0) + \tfrac{1}{2}\, V(1)$$

$$U(M) = \tfrac{1}{2}\, V(M-1) + \tfrac{1}{2}\, V(M)$$

Thus we have arrived at the final estimate $V(R)$ for power at frequency $\frac{R}{2M\Delta t}$ (positive frequencies only; single sided spectrum).

Accuracy and Record Length

Blackman and Tukey approach this subject by introducing equivalent degrees of freedom, a statistically useful but physically not very satisfying concept. Consequently, we shall merely indicate a useful formula and direct those interested in further detail to Blackman and Tukey, Section B23.

The record length, $T_n = N\Delta t$, is a function of the accuracy, confidence level, frequency resolution, and number of pieces (if the record has been interrupted in one or more places). The accuracy A is specified in db for a confidence level (80% here). The resolution in Hertz is just the reciprocal of the maximum lag, $M\Delta t$. The record length then is

$$Tn = \tfrac{1}{2} + \frac{125}{(A\ db)^2} + \frac{Pieces}{3} \cdot \frac{1}{M\Delta t} \quad .$$

REFERENCES

1. D.A. Bell, Electrical Noise: Fundamentals and Physical Mechanisms. Princeton: Van Nostrand, 1960.

2. A. Van der Ziel, "On the Noise Spectra of Semiconductor Noise and of Flicker Effect," Physica, vol. 16 (April, 1950), p. 359.

3. Staff, "Reviewing Recent Developments in Electronics," EEE, vol. 17 (July, 1969), p. 48.

4. D. Wolf, and E. Holler, "Bistable Current Fluctuations in Reverse-Biased p-n Junctions in Germanium," Journal of Applied Physics, vol. 38 (January, 1967), p. 189.

5. W.H. Card, and P.K. Chaudhari, "Characteristics of Burst Noise," Proceedings of the IEEE, vol. 53 (June, 1965), p. 652.

6. S.T. Hsu, and R.J. Whittier, "Characterization of Burst Noise in Silicon Devices," Solid State Electronics, vol. 12 (November, 1969), p. 867.

7. R.C. Bean, "Evidence for Multiple Conductance Levels in the Cation Permeable Channels of Lipid Bilayer Membranes with Negative Resistance," unpublished.

8. H.A. Haus, et al., "Representation of Noise in Linear Twoports," Proceedings of the IEEE, vol. 48 (January, 1960), p. 69.

9. P.L. Leonard, and S.V. Jaskolsky, "An Investigation into the Origin and Nature of 'Popcorn Noise'," Proceedings of the IEEE, vol. 57 (October, 1969), p. 1786.

10. _____, "Microplasma Model for 'Popcorn Noise'," IEEE International Electron Device Meeting, Washington, D.C., October, 1969.

11. R.H. Haitz, et al., "Avalanche Effect in Silicon p-n Junctions. I - Localized Photomultiplication Studies on Microplasmas," Journal of Applied Physics, vol. 34 (June, 1963), p. 1581.

12. A.S. Grove, Physics and Technology of Semiconductor Devices. New York: J. Wiley and Sons, 1967.

13. S.T. Hsu, R.J. Whittier, and C.A. Mead, "Physical Model for Burst Noise in Semiconductor Devices," International Electron Device Meeting, Washington, D.C., October, 1969.

14. A. Papoulis, Probability, Random Variables, and Stochastic Processes. New York: McGraw-Hill, 1965.

15. R.B. Blackman, and J.W. Tukey, The Measurement of Power Spectra from the Point of View of Communications Engineering. New York: Dover, 1959.

16. A. Van der Ziel, Fluctuation Phenomena in Semiconductors. London: Butterworths, 1959.

17. J.R. Carson, "The Statistical Energy-Frequency Spectrum of Random Disturbances," Bell System Telephone Journal, vol. 10 (July, 1931), p. 374.

18. W. Magnus, and F. Oberhettinger, Formulas and Theorems for the Functions of Mathematical Physics. New York: Chelsea, 1949.

REFERENCES NOT SPECIFICALLY CITED

C.A. Bittman et al., "Technology for the Design of Low Power Circuits," IEEE Journal of Solid State Circuits, vol. 5 (Feb., 1970), p. 29.

G. Giralt, et al., "Le Bruit en Creneaux des Transistors Plans au Silicium," Electronics Letters, vol. 2 (June, 1966), p. 228.

C.A. Mead, "Metal-Semiconductor Surface Barriers," Solid State Electronics, vol. 9 (Nov./Dec., 1966), p. 1023.